Chair of Geoenergy Production Engineering

Master's Thesis
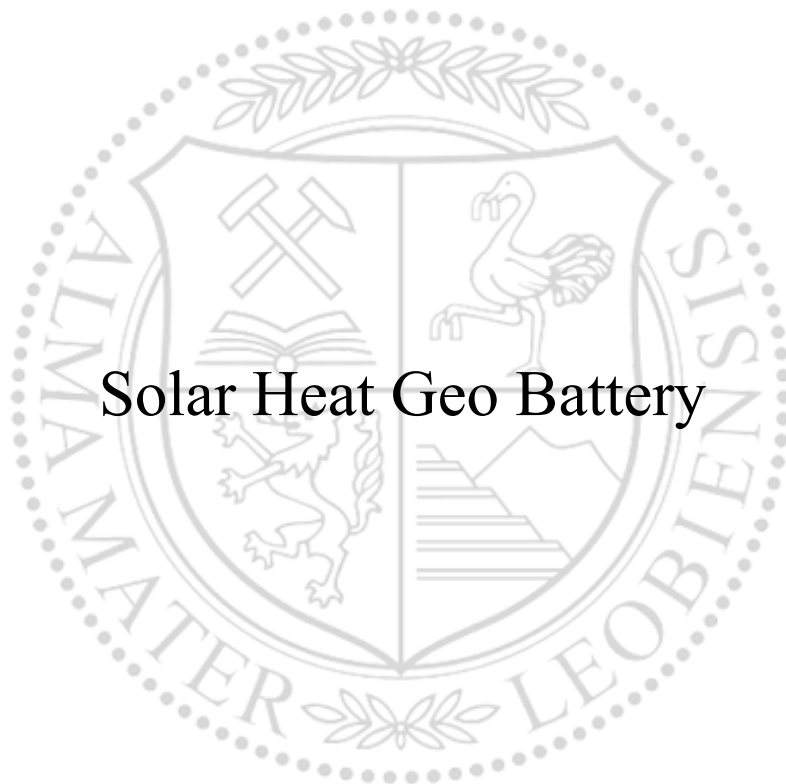
Solar Heat Geo Battery

Clara Maria Kopeinig, BSc

November 2024

MONTANUNIVERSITÄT LEOBEN
www.unileoben.ac.at

EIDESSTATTLICHE ERKLÄRUNG

Ich erkläre an Eides statt, dass ich diese Arbeit selbstständig verfasst, andere als die angegebenen Quellen und Hilfsmittel nicht benutzt, den Einsatz von generativen Methoden und Modellen der künstlichen Intelligenz vollständig und wahrheitsgetreu ausgewiesen habe, und mich auch sonst keiner unerlaubten Hilfsmittel bedient habe.

Ich erkläre, dass ich den Satzungsteil „Gute wissenschaftliche Praxis" der Montanuniversität Leoben gelesen, verstanden und befolgt habe.

Weiters erkläre ich, dass die elektronische und gedruckte Version der eingereichten wissenschaftlichen Abschlussarbeit formal und inhaltlich identisch sind.

Datum 29.10.2024

Unterschrift Verfasser/in
Clara Maria Kopeinig

Clara Maria Kopeinig
Master Thesis 2024
Geoenergy Engineering

Solar Heat Geo Battery

Supervisor: Univ.-Prof. Keita Yoshioka, PhD
Co-Supervisor: Chaofan Chen, Dr. rer. nat.

Chair of Geoenergy Production Engineering

Acknowledgments

I would like to express my sincere gratitude to my supervisor, Univ.-Prof. Keita Yoshioka, PhD, for his guidance and support throughout the course of my thesis. His insights and encouragement have been instrumental in shaping this thesis. I am also deeply grateful to my co-supervisor, Chaofan Chen, Dr. rer. nat., for his constructive feedback and technical guidance, which greatly enriched the depth and rigor of this thesis.

Furthermore, I would like to express my sincerest gratitude to my husband, Jacob, for his constant support, patience, and assistance.

Abstract

With the significant development of renewable energy sources such as solar and wind power, energy systems are increasingly challenged by the mismatch between energy supply and demand. Photovoltaic systems, for example, often generate excess energy during peak sunshine hours, particularly in summer, which do not match with the periods of highest energy demand. This intermittent generation creates a need for robust thermal energy storage that can store the surplus of energy and release it as needed. Several types of underground thermal energy storage systems are currently being used to meet energy storage needs. The main underground thermal energy storage system technologies include aquifer thermal energy storage, borehole thermal energy storage and pit thermal energy storage. A significant gap remains when it comes to developing a controlled approach to thermal energy storage within aquifers that can store heat without fluid injection, where a geothermal reservoir is artificially created by heating it using renewable energy. To address this gap, this study investigated the creation of an artificially heated geothermal reservoir by installing a solar powered resistive heating rod. In this approach, heat is stored in situ within the aquifer, allowing for stable and localized storage. Using OpenGeoSys, a numerical model was developed to simulate heat transfer in a 2D subsurface environment, capturing both conduction and convection mechanisms. Key parameters have been subject to a sensitivity analysis, including permeability, porosity, groundwater flow velocity, thermal dispersivity and the specific heat capacity and thermal conductivity of sandstone to evaluate their impact on heat propagation, storage efficiency and thermal plume development. This modelling effort provides insight into the feasibility of storing thermal energy in aquifers heated by a heating rod and provides a basis for designing systems capable of efficiently recovering stored thermal energy, particularly in seasonal storage applications.

Zusammenfassung

Die rasche Entwicklung erneuerbarer Energiequellen wie Solar- und Windenergie führt, aufgrund des Ungleichgewichts zwischen Energieangebot und Nachfrage, zu wachsenden Herausforderungen. Beispielsweise erzeugen Photovoltaikanlagen in Zeiten hoher Sonneneinstrahlung, insbesondere im Sommer, häufig überschüssige Energie, während in Zeiten, in denen nicht genügend Energie erzeugt werden kann, ein erhöhter Bedarf besteht. Dies führt zu einem Bedarf an robusten thermischen Energiespeichern, die überschüssige Energie speichern und bei erhöhter Nachfrage abgeben können. Derzeit werden verschiedene Arten von unterirdischen thermischen Energiespeichersystemen eingesetzt. Zu den wichtigsten Technologien gehören die thermische Energiespeicherung in Aquiferen, die thermische Energiespeicherung in Bohrlöchern und die thermische Energiespeicherung in Minen. Eine wesentliche Lücke besteht noch bei der Entwicklung eines kontrollierten, geschlossenen Kreislaufs für die thermische Energiespeicherung in Aquiferen, der Wärme ohne Injektion von Flüssigkeiten speichern kann, wobei eine geothermische Lagerstätte durch Aufheizen mit erneuerbarer Energie künstlich geschaffen wird. Um diese Lücke zu schließen, wurde in dieser Studie eine künstlich erwärmte geothermische Lagerstätte durch den Einbau eines solarbetriebenen Widerstandsheizstabes untersucht. Bei diesem Ansatz wurde die Wärme vor Ort im Aquifer gespeichert, was eine stabile und lokale Speicherung ermöglicht. Unter Verwendung von OpenGeoSys wurde ein numerisches Modell entwickelt, um die Wärmeübertragung in einer 2D-Umgebung im Untergrund zu simulieren, wobei sowohl konduktive als auch konvektive Mechanismen berücksichtigt werden. Die wichtigsten Parameter wurden einer Sensitivitätsanalyse unterzogen, darunter Permeabilität, Porosität, Fließgeschwindigkeit des Grundwassers, thermische Dispersivität sowie spezifische Wärmekapazität und Wärmeleitfähigkeit des Sandsteins, um ihren Einfluss auf die Wärmeausbreitung und Speichereffizienz zu bewerten. Diese Modellierung gibt Aufschluss über die Machbarkeit der Wärmespeicherung in Aquiferen in einem geschlossenen Kreislauf und bildet die Grundlage für die Entwicklung von thermischen Energiespeichersystemen, die die gespeicherte Wärmeenergie insbesondere für saisonale Speicheranwendungen effizient zurückgewinnen können.

Table of Contents

xii

Chapter 1

Introduction

Thermal Energy Storage (TES) gains importance in meeting the challenges posed by fluctuating energy demand and the intermittent nature of renewable energy sources such as solar energy. As global energy consumption continues to rise, the integration of renewable energy into the grid has become essential to reduce greenhouse gas emissions and minimize dependence on fossil fuels. However, renewable sources are inherently variable, with solar only available during the day and wind inconsistent. This variability creates challenges in maintaining a steady and reliable supply of energy. TES plays a key role in overcoming these challenges by decoupling energy generation from consumption. This ensures that energy is available even in times when renewable sources are not actively producing power. The importance of TES extends beyond power generation, as it also plays an important role in heating and cooling applications. In many regions the demand for heating and cooling accounts for a significant proportion of energy consumption(Stoppato and Benato, 2017).

This thesis investigated a numerical model of a TES system within an artificially heated geothermal aquifer, developed using the OpenGeoSys simulation platform. Unlike conventional Aquifer Thermal Energy Storage (ATES) systems, where hot water is injected into the aquifer to store heat, the system modelled in this study adopted a configuration where the water is heated by an external heat source but remains confined within the system without exchanging with the surrounding groundwater. The primary objective of this research was to assess the viability of the TES system for geothermal energy extraction in both the short and long term. In this context, the model examined whether the heat propagates sufficiently far within a feasible time scale to ensure efficient heat transport. By simulating the heat distribution and storage behavior within the porous medium, this study aimed to demonstrate how thermal energy propagates through the aquifer and lay the groundwork for future research to assess the potential for recovery via a geothermal doublet system. The Thesis includes an investigation of

key parameters such as thermal diffusivity, permeability and porosity of the porous medium, which govern the heat transfer dynamics within the system. Thermal Parameters of the Sandstone as well as groundwater flow velocities have also been investigated. By integrating theoretical research and numerical modelling, this study aims to contribute to the understanding of a geothermal TES systems and their application in large-scale energy storage.

1.1   Background and Context

There are several different methods and options for storing energy. This thesis focuses on TES, specifically Underground Thermal Energy Storage (UTES), where energy is stored as heat. TES can be described in terms of three main technologies. Sensible heat storage functions by means of temperature changes of a material, with the energy stored being proportional to the temperature difference. Latent heat storage involves the altering the phase of a material, typically from solid to liquid or the other way around, where the temperature remains constant, and the stored energy depends on the latent heat of fusion of the material. Thermochemical heat storage, on the other hand, involves storing heat in chemical compounds formed by an endothermic reaction. The energy is then retrieved by an exothermic reaction that recombines these compounds, with the stored energy equal to the heat of the reaction(Stoppato and Benato, 2017).

1.2   Scope and Objectives

This study focused on the simulation of heat transfer in subsurface porous media, using OpenGeoSys. The main objective was to investigate how heat is transferred through an artificially created geothermal aquifer, considering the different roles of conduction and convection depending on the permeability and porosity conditions. The numerical model simulated heat transport in UTES systems, with particular emphasis on how different geological configurations, such as low-permeability clay layers and high-permeability aquifers, affected the efficiency of heat distribution and storage.

The scope of the study encompasses the construction of a detailed numerical model in OGS that represents a multi-layered geological system where a heat source interacts with subsurface porous media. The model analyzed heat transfer by conduction and convection in higher permeability aquifer regions, simulating conditions relevant to UTES. In addition, the study investigated how hydrogeological parameters such as porosity, permeability, thermal conductivity, specific heat capacity, thermal dispersivity and groundwater flow influence heat transport mechanisms within the subsurface.

1.3   Achievements

This study has successfully developed a numerical model using OGS to simulate heat transfer within a 2D subsurface aquifer system, focusing on both conduction and convection mechanisms. The model accurately represents subsurface heat transfer processes under varying conditions. The OGS HT process benchmark, validated through analytical solutions and real-world applications, has been used to ensure accuracy. Due to the robustness of the OGS HT benchmark, no external field validation data was required as the benchmarked process is widely recognized for its reliability in modelling hydro-thermal interactions in subsurface environments.

A sensitivity analysis was conducted to evaluate the effect of key parameters on heat transfer. This analysis provided a profounder understanding of how these parameters influence the thermal behavior of the aquifer, allowing the model to be refined and ensuring its applicability to different geological settings.

1.4   Technical Issues

An unresolved technical issue in this study relates to the accuracy of the HT process at higher temperatures. If the temperature in the system rises above a certain threshold value, the current model may no longer accurately represent the thermal dynamics because it does not account for potential phase changes in the water, from liquid to vapor and vice versa. These phase transitions would significantly affect the heat transfer process, requiring a more complex model to account for latent heat and the associated energy exchanges. Since the model employed in this study does not account for these phase changes, its accuracy is limited as temperatures approach levels where such phase changes could occur.

1.5   Overview of Thesis

The initial chapter presents the necessity for this research, which is driven by the growing need for efficient TES systems to address the mismatch between energy supply and demand, especially in renewable energy systems. Chapter 2, the state of the art, reviews existing technologies related to UTES and photovoltaic systems, highlighting the role of geothermal systems in energy storage.

Chapter 3 details the methodology, focusing on the development of a numerical model using OGS to simulate the transfer of heat by conduction and convection in a 2D aquifer system. A sensitivity analysis was carried out to assess the effect of key parameters heat storage performance of the system.

Chapter 4 presents the results and discussion, evaluating the results of the sensitivity analysis and comparing the findings with previous studies. Key findings on how these parameters affect energy storage are discussed, including the role of temperature dependent material properties. In conclusion, Chapter 5 presents a summary of the contributions made by the study.

Chapter 2

State of the Art

2.1 Underground Thermal Energy Storage

UTES has become an important technology for improving the efficiency of renewable energy use, particularly in areas where there are substantial seasonal variations in energy demand. By transferring heat from the warmer months to the colder months, UTES helps to bridge the temporal gap between energy supply from solar sources, and energy demand. This technology is essential for promoting energy conservation and the wider adoption of renewable energy systems. Despite its potential, UTES faces several challenges that limit its widespread adoption. One of the key problems is the significant heat loss associated with large-scale systems, resulting in lower-than-expected efficiencies. Selecting suitable materials for long-term energy storage, developing effective insulation strategies and optimizing system designs to minimize heat loss remain significant hurdles(Zhou, 2021).

Kallesøe et al. (2021) describe in their paper different types of UTES, state of the art technologies, example cases and lessons learned. Four main types of UTES are discussed and described. The technologies covered are high temperature aquifer thermal energy storage, borehole thermal energy storage (BTES), mine thermal energy storage (MTES) and pit thermal energy storage (PTES). High temperature ATES works by injecting and later withdrawing heated water into aquifers located in both shallow and deep geological formations. These aquifers can consist of unconsolidated sand, porous rocks such as sandstone or limestone, or even fractured geological formations. Systems operating at injection temperatures above 60°C are classified as high temperature ATES, while medium temperature ATES systems operate within a temperature range of 30°C to 60°C. BTES stores thermal energy in underground soil or rock formations using their high natural heat capacity. The subsurface is heated using closed loop borehole heat exchangers installed in large numbers with a span of 2-5m to efficiently heat

the subsurface. The heat can then be extracted for later use also by borehole heat exchangers. Temperatures up to 90°C can be successfully stored. The working principle of PTES is based on hot water stored in large, excavated pits insulated by a cover. The pit is lined with polymers or concrete. One of the advantages of PTES is the fast charging and discharging times and the fact that it can be used for short storage periods. Although this option requires a larger footprint, the construction costs are low compared to the other options. MTES uses abandoned water-filled mines as thermal reservoirs. Although still largely experimental, MTES offers a promising approach to reusing old industrial sites for energy storage(Kallesøe *et al.*, 2021).

TES systems for solar energy are characterized by six key factors. Capacity refers to the amount of energy the system can store, which depends on the storage process, the medium used and the size of the system. Performance indicates how quickly the stored energy can be either discharged or recharged. Efficiency measures the effectiveness of the system by comparing the energy provided to the user with the energy required to charge the system, considering any losses during the storage period and the charge/discharge cycle. The storage period defines the length of time the energy can be stored and can vary from hours to months, making it suitable for seasonal storage. The charge and discharge times are the times needed to fully charge or discharge the system. Finally, cost refers to the cost of capacity (€/kWh) or power (€/kW), which is influenced by both the initial investment and operating costs, as well as the predicted lifetime of the system and the number of cycles it is able to perform (Sarbu and Sebarchievici, 2018).

The research on UTES by Zhang et al. (2024) has categorized the technology into three main systems: ATES, BTES and Cavern Thermal Energy Storage (CTES). Each system has developed along different paths, influenced by factors such as geological conditions, technological advances and economic considerations. ATES, which involves storing energy in confined aquifers, is one of the most mature and widely deployed UTES technologies. It has been widely adopted in countries with favorable geological conditions and has demonstrated significant potential for energy savings and reduced dependence on fossil fuels. However, ATES faces challenges such as wellbore scaling, corrosion and injection plugging, which can reduce system efficiency and lifetime. BTES, which uses buried pipes to store thermal energy in the ground, has also seen significant development. This system is more versatile than ATES because it does not depend on specific aquifer conditions, making it suitable for a wider range of sites. BTES has been successfully implemented in various projects around the world, including Canada and Europe, where it is often combined with other renewable energy technologies such as solar panels. The main challenges with BTES include managing heat loss through conduction and ensuring the economic viability of the system. CTES, which uses natural or man-made underground caverns to store thermal energy, is less common due to the

specific geological requirements and high costs associated with its implementation. CTES has significant benefits in terms of storage capacity and efficiency, particularly in regions where large-scale energy storage is required. Multi-energy coupling, which integrates UTES with other renewable energy sources, increases the overall efficiency and flexibility of energy systems, enabling better management of energy supply and demand. Economically, UTES technologies, particularly ATES and BTES, offer favorable advantages over traditional energy storage methods. They have the potential to decrees energy costs and greenhouse gas emissions, contributing to global efforts to combat climate change. However, the economic feasibility of UTES is highly dependent on local settings, including the accessibility of suitable geological formations and the existence of supportive government policies(Zhang *et al.*, 2024).
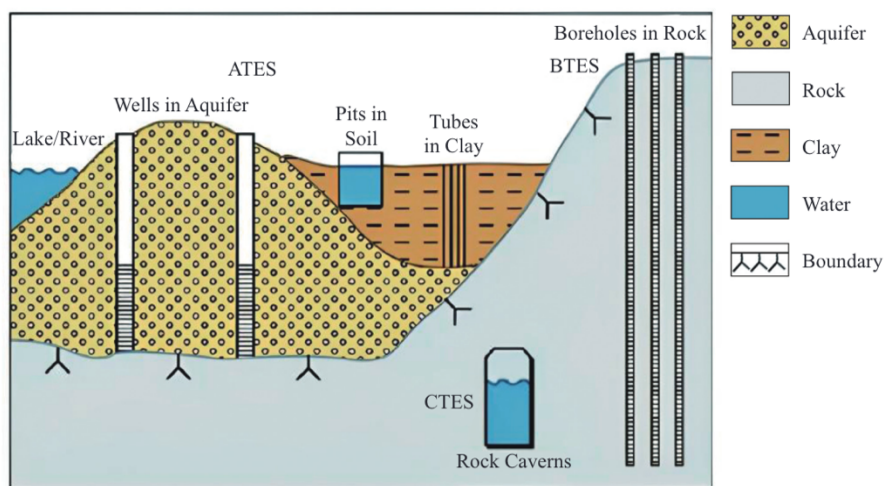
Figure 1- UTES systems(Zhang et al.*, 2024, p. 93)*

2.2   Photovoltaic Systems and Energy Production Potential

As photovoltaic (PV) technology was considered as the primary energy source for heating the aquifer in this study, it is important to understand its basic principles and operation. This chapter provides a brief overview of PV technology, including its operating principles, system components and key factors affecting performance. By understanding the basics of PV energy generation, its role in supporting thermal energy storage can be assessed.

Solar energy is recognized as a promising solution to the world's increasing energy needs which are driven by population growth and technological advances. Solar energy is highly sustainable due to its abundant availability and cost effectiveness, especially when compared to other renewable resources. The technology has developed significantly with improvements in

photovoltaic systems, which convert sunlight into electricity. PV technology focuses on the direct conversion of sunlight into electricity without the need for intermediaries. This technology primarily uses semiconductors to induce the movement of electrons, creating an electric current. Recent advances have focused on increasing the efficiency of PV panels through various techniques, including solar tracking systems that improve the capture of solar radiation. Despite these advances, the solar industry faces several barriers, including high manufacturing costs, environmental factors affecting performance, and the need for improved awareness and infrastructure. Continued research and development aims to overcome these challenges and further promote solar energy as a key player in the global energy transition(Kannan and Vakeesan, 2016).

A typical PV cell consists of a p-n junction made of semiconductor materials, usually silicon. When sunlight reaches the surface of the cell, photons excite electrons within the semiconductor, triggering them to jump from the valence band (low-energy state) to the conduction band (high-energy state). This motion creates electron-hole pairs. The built-in electric field at the p-n junction drives the electrons to the n-type side and the holes to the p-type side, creating a flow of electric current. This current is then captured and passed through an external circuit to produce usable electrical power. The efficiency of this process is influenced by factors such as material quality, light absorption and cell design(Green, 2002).

The output of a PV system is determined by several key factors, including solar irradiance, system design and efficiency. Solar irradiance, the amount of sunlight received per square meter at any given site, is one of the key factors determining the energy output of any PV installation. Irradiance values can be categorized into three main types: Global Horizontal Irradiance, which is the total solar radiation on a horizontal surface, Direct Normal Irradiance, which measures direct solar radiation and Diffuse Horizontal Irradiance, which accounts for radiation scattered by the atmosphere (Usman *et al.*, 2020). Each location on earth has unique irradiance values that must be considered during the design process to ensure accurate performance predictions. To estimate the energy output of a PV module, the following equation is typically used:

$$\eta_{pv} = \eta_{ref}\{1 - a[((G_B)/18) + T_A - 20]\} \qquad\qquad 1$$

$$W_p = \eta_{pv} G_B A \qquad\qquad 2$$

where W_p is the maximum power output (in watts), *a* represents a power correction factor of 0.0042, η_{pv} is the efficiency of the PV module, G_B is the solar irradiance (in kW/m²), and *A* is the area of the module. This equation provides a direct means of calculating the power output

of the system under ideal conditions, considering the efficiency of the PV cells and the solar energy available at a given location. Modules with higher efficiencies, such as monocrystalline silicon cells, perform better but tend to be more expensive than alternatives such as polycrystalline or thin-film modules. Larger arrays capture more solar energy, increasing power output. However, real-world performance is affected by external factors, with the Performance Ratio measuring the efficiency of the system. The Performance Ratio, typically between 0.75 and 0.85, considers inefficiencies such as shading, temperature effects and component losses. Factors such as dust, poor installation and incorrect module orientation can reduce energy output by up to 30%. Shading, even partial, has a significant impact on performance, reducing output and potentially damaging cells. Sunshine hours, which vary by location, are critical in estimating energy production, with systems in sunnier areas producing more energy. Proper system design, including module selection, inverter sizing and battery capacity, is key to optimizing performance. The orientation and the tilt angle of the modules, ideally close to the latitude of the site, will also affect sunlight capture and energy yield(Usman *et al.*, 2020).

Chapter 3

Methodology

3.1   Model Conceptualization

The numerical simulation developed in this thesis used the OpenGeoSys (OGS) framework, specifically the Hydro-Thermal (HT) process to model heat transfer mechanisms within a porous geothermal reservoir. The focus of the model was a subsurface system located between 800- and 1100 meters depth, which consisted of three distinct layers: an upper and a lower aquiclude layer, each 100 meters thick, and an aquifer located between 900 and 1000 meters. The width of the simulation domain was 800 meters. The aquifer layer served as the primary zone for thermal energy storage, with a constant Dirichlet boundary condition of 300°C (573.15K) applied to simulate a 50m long heat source at the bottom of the aquifer.
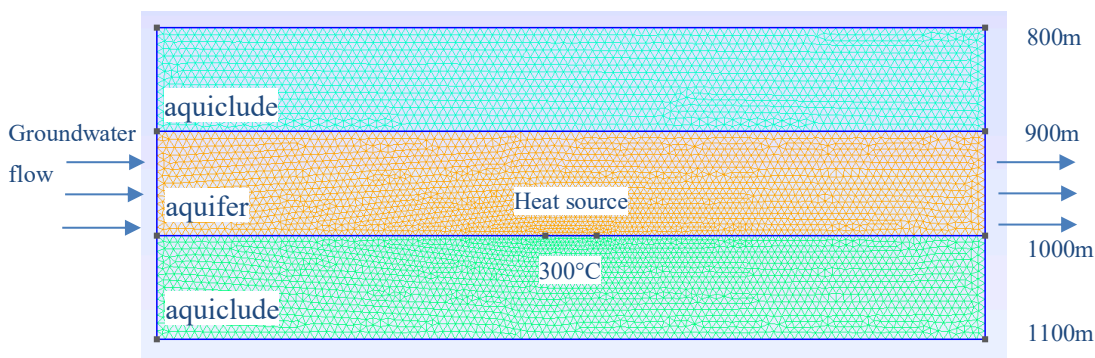
Figure 2 - TES model

The simulation focused on capturing the heat distribution throughout the system. This analysis assisted in the creation and evaluation of an artificially created high temperature geothermal reservoir. The aim was to determine whether a large enough thermal area can be created within the aquifer in a feasible time frame to allow energy production through geothermal extraction. By understanding how heat propagates through the system, the simulation evaluated whether

the stored thermal energy can be efficiently harnessed for future geothermal power generation using a geothermal doublet.

The heat source simulated in the model was a metal heating element that works on the principle of resistive heating. This works by passing an electric current through a conductor with inherent resistance, such as a metal alloy. As the current flows, the resistance impedes the movement of electrons which converts electrical energy into heat. The heat generated is proportional to the square of the current and the resistance. This principle is widely used in heating elements to provide efficient and controlled heat transfer(EEP-Electrical Engineering Portal and Csanyi, 2011).

In addition to the simulation, a sensitivity analysis was performed to investigate the influence of several material and system properties on the heat transfer behavior. This study systematically varied key properties such as thermal conductivity, permeability, porosity, groundwater velocity, thermal dispersivity and specific heat capacity. Each variable played an important role in the thermal response of the system. The sensitivity analysis provides insight into how different geological conditions could affect the efficiency of heat storage and transfer in the UTES systems. By adjusting the properties of each layer and the dynamics of groundwater flow, the model assessed the feasibility of using this system for TES, particularly in the context of geothermal energy extraction through a geothermal doublet in the future. This approach ensures that the model is robust over a range of realistic geological conditions and provides a comprehensive understanding of the system's potential for large-scale, long-term TES applications.

In this study, the aquifer was heated to temperatures of up to 300°C. At these temperatures, both the density and viscosity of the water vary significantly, and these variations have a critical influence on the convective movement of water within the aquifer. To accurately model these temperature dependent properties, CoolProp was used to obtain both density and viscosity values of water. CoolProp is an open-source library designed to calculate thermophysical properties of fluids with high accuracy over a wide range of conditions(Bell *et al.*, 2014). It was particularly suitable for this project due to its extensive validation against experimental data and its use of robust thermodynamic models, such as the IAPWS-97 formulation for water and steam (IAPWS, 1997). This ensured that the viscosity and density values obtained are reliable even at elevated temperatures, making CoolProp a good choice for geothermal simulations (Bell et al., 2014). To incorporate the temperature dependent changes in viscosity and density into the simulation, a Python code was written to use CoolProp for these properties over the relevant temperature range. The data obtained was then plotted in Excel to visualize the trends. For both viscosity and density, trendlines were generated from the plotted data and the

corresponding equations were extracted. These trendline equations were then implemented into the OpenGeoSys project to account for the temperature dependent behavior of water. This allowed the simulation to accurately capture the dynamics of fluid movement within the porous medium of the geothermal aquifer. The implementation of these properties was critical because, at high temperatures, reduced viscosity leads to reduced resistance to flow, while temperature-induced changes in density drive convective circulation. The temperature dependent behavior of water density and viscosity is shown in Figure 3 and Figure 4.
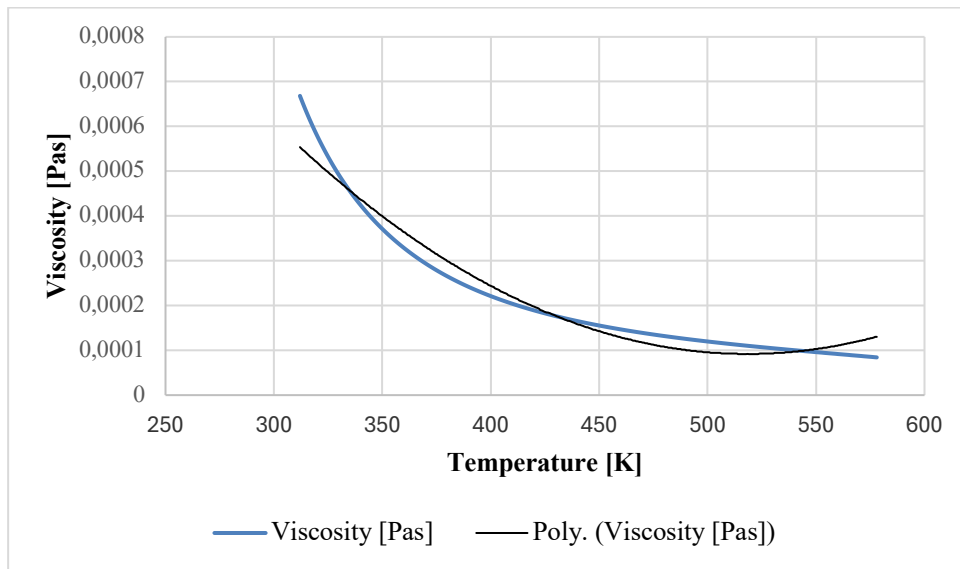
Figure 3 Temperature dependent water viscosity and polynomial fitted trendline

In the OpenGeoSys simulation, the temperature dependence of the water density is implemented using a linear relationship. The density $\rho(T)$ is defined as

$$\rho_f(T) = \rho_{ref}(1 - \beta(T - T_{ref}))$$

3

Where ρ_{ref} is the reference density at the reference temperature $Tref$ and β is the coefficient of thermal expansion. This formulation captures the decrease in water density with increasing temperature, which is a key driver of natural convection in geothermal systems. In the model, this effect was critical for simulating the flow behavior in the aquifer, where heated, less dense water rises and cooler, denser water sinks, forming convective currents and having a significant impact on the final heat distribution, which was of interest in observing the feasibility of constructing an artificial geothermal system. To ensure that the simulation correctly reflects the

real-world behavior of water in the temperature range relevant to the geothermal system, the coefficient of thermal expansion was obtained from a linear trend line fit to the density values generated by CoolProp (Figure 4). This approach provided a realistic coefficient of thermal expansion for the specific temperature range of the aquifer, ensuring that the density variation, and hence the induced convection, was modelled as accurately as possible. The inclusion of temperature-dependent density in the simulation allowed more accurate predictions of buoyancy-driven flow, which is essential for understanding heat transport and flow dynamics in geothermal reservoirs.
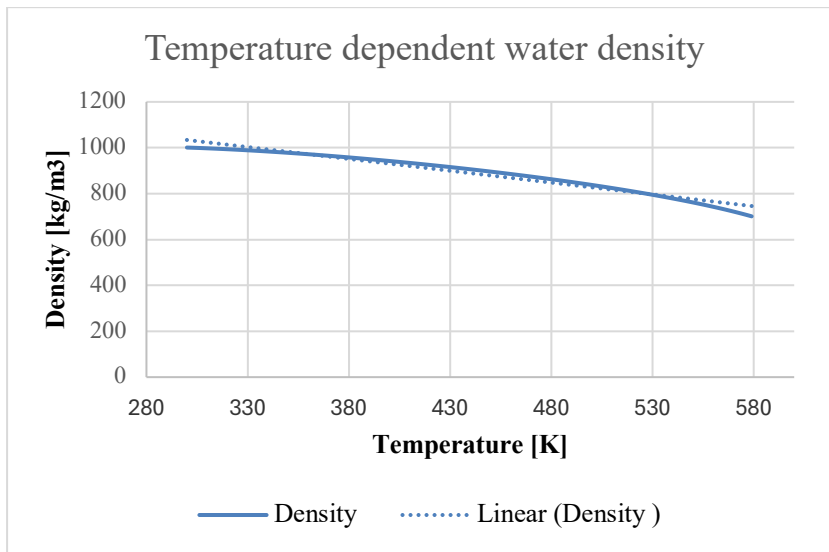
Figure 4 Temperature dependency of water density and linear fitted trendline

3.2   Software Overview

OpenGeoSys (OGS) is an open-source platform for the simulation of hydro-thermal processes in porous and fractured media. It is widely used in areas such as geothermal energy systems, hydrology, CO_2 sequestration and nuclear waste disposal. OGS uses the Finite Element Method to solve coupled physical processes such as heat transfer, groundwater flow and chemical transport. Its modular design allows users to customize simulations for different environmental and geotechnical challenges(Naumov *et al.*, 2024).

The HT (Hydro-Thermal) process in OGS formed the basis for simulating heat transport in porous media, specifically combining thermal and groundwater flow. The HT process is modelled by parabolic partial differential equations that describe how heat moves via thermal gradients, conduction, and fluid movement, advection. The core of the simulation is governed

by balance equations that account for heat accumulation and transfer by both conductive and advective processes. This is key to modelling the vertical and horizontal distribution of heat in the system. The combined effects of conduction, described by Fourier's law, and advection, driven by groundwater flow and density changes, ensure that both forms of heat transport in the aquifer are accurately captured. Advective heat transfer depends on fluid movement within the aquifer, described by Darcy's Law, which includes the effects of fluid viscosity and density, both depending on temperature. These dependencies ensure that heat transfer by advection adjusts to changes in temperature within the aquifer. In addition, the model uses the heat conduction equation, based on Fick's law, to capture thermal diffusion through both the solid and fluid parts of the system. The interaction between the fluid flow and the porous media leads to thermal dispersion, which also affects the propagation of heat throughout the reservoir. Finite element discretization was used to solve these equations, dividing the spatial domain into small elements. Each element uses shape functions to approximate the temperature distribution across the domain, allowing accurate numerical solutions. This discretization is particularly useful for simulating complex geometries such as the layered structure of the system, which consists of aquiclude and aquifer layers. The HT method also incorporates temperature-dependent fluid properties, such as density and viscosity, to model the interaction between heat and groundwater flow. As temperature increases, fluid density decreases, leading to buoyancy-driven flow, which can significantly influence vertical heat movement. This coupling of heat and fluid flow is treated using the Boussinesq approximation, which simplifies the system by assuming that changes in density primarily affect buoyancy forces(Fischer *et al.*, 2017).

3.3   Governing Equations

This section presents the fundamental governing equations used in the simulation, detailing how the HT process captures the coupled behavior of heat transfer and groundwater flow within a porous geothermal system. The equations are essential for modelling heat distribution and fluid movement and provide the basis for assessing the thermal performance and energy storage potential of the system.

To facilitate numerical simulation, the governing equations are transformed into their weak form using the Finite Element Method. This transformation involves integrating the equations over the domain and applying the Galerkin method, which allows accurate discretization of the heat and fluid flow processes. The weak formulation ensures that the numerical model can deal efficiently with complex geometries and varying material properties, which is the key to the simulation of realistic subsurface conditions.

The following equations were taken from the OGS HT benchmark paper by Fischer et al. (2017), which outlines HT processes in porous media, including key equations related to balance equations, groundwater flow and heat transfer using OGS (Fischer *et al.*, 2017).

3.3.1 Heat and Mass Balance Equation

The HT process starts with a general balance equation that describes how heat or mass changes over time within a given domain. This balance is affected by heat accumulation, heat flux across domain boundaries, and internal sources or sinks. The general form of the equation is:

$$\frac{\partial}{\partial t}\int_{\Omega} S\big(T(x,t)\big)dx = -\int_{\Gamma}\langle J(x,t)|n(x)\rangle d\sigma + \int_{\Omega} Q(x,t)dx \qquad 4$$

Here, *T(x,t)* represents the quantity of interest, in this case heat, *S(u)* is its storage term, *J(x,t)* represents the flux, the flow of heat or fluid, and *Q(x,t)* represents any internal sources or sinks. Applying the Gauss theorem to this equation, it can be rewritten in the differential form:

$$\frac{\partial S(T(x,t))}{\partial t} + div\, J(x,t) - Q(x,t) = 0 \qquad 5$$

This forms the basis for both the heat transport and groundwater flow equations.

Heat transport within the porous medium involves two main processes: conduction and advection. The Fourier law describes conductive heat flow as follows:

$$J_{cond} = -K\nabla T \qquad 6$$

where *K* is the thermal conductivity of the medium and *T* is the temperature. For advective heat transport, the flux is driven by the velocity of the fluid flow, described as:

$$J_{adv} = cT \qquad 7$$

where c is the velocity vector of the fluid. When these processes are combined, the resulting heat transport equation in its parabolic partial differential equation form becomes:

$$\frac{\partial S(T(x,t))}{\partial t} - \nabla \cdot [K(x,t)\nabla T(x,t) - cT(x,t)] - Q(x,t) = 0 \qquad\qquad 8$$

This equation captures how temperature evolves over time, considering both diffusion and advection in the presence of fluid flow.

3.3.2 Groundwater Flow

Darcy's Law is used to model the flow of ground water through the porous medium. This law describes fluid movement due to pressure gradients and gravitational forces, which are influenced by the temperature. The velocity of the fluid, q, is given by:

$$q = -\frac{\kappa}{\mu(T)} grad\ \psi \qquad\qquad 9$$

where κ is the intrinsic permeability tensor of the porous medium, $\mu(T)$ is the dynamic viscosity of the fluid and Ψ is the hydraulic potential, defined as

$$\Psi = p + \rho_f(T)gz \qquad\qquad 10$$

Where p is the pressure, $\rho_f(T)$ is the temperature dependent density of the fluid and gz is the gravitational effect. The combination of pressure gradients and buoyancy effects due to temperature variations drives groundwater flow within the aquifer.

In the groundwater flow equation, the storage function S in the balance equation is replaced by $\phi\rho\ (x,\ t,\ p)$ where ϕ is the porosity. This modification considers the fact that the fluid density ρ_f depends on the pressure p and the temperature T. The equation is given as

$$\frac{\partial \phi\rho(p,T)}{\partial t} - div\frac{\kappa}{\mu(T)} grad\ \Psi - Q(x,t) = 0 \qquad\qquad 11$$

Internal sources or sinks are described by $Q(x,t)$, which can arise from changes in, for example, temperature. Assuming an incompressible medium, the porosity is constant. The Boussinesq approximation simplifies the equation by neglecting the temperature terms which results in a new form of the mass balance equation. This leads to the final expression:

$$S\frac{\partial p}{\partial t} - div\left[\frac{\kappa}{\mu(T)}grad\ \psi\right] - Q(x,t) = 0 \qquad\qquad 12$$

3.3.3 Heat Conduction

Heat conduction is modelled by Fick's law, where the heat flow J is proportional to the diffused quantity, in this case the Temperature T. The hydrodynamic thermodispersion tensor is described as λ

$$J = -\lambda\ grad\ T \qquad\qquad 13$$

3.3.4 Coupled Heat and Fluid Flow

The HT process links heat transport and fluid flow, meaning that changes in fluid temperature directly affect fluid density and viscosity, which in turn affect fluid movement through Darcy's Law. The resulting heat transfer equation, which includes both the diffusion and the advection terms, can be expressed as follows:

$$c_p\frac{\partial T}{\partial t} - div\ (\lambda grad\ T) + \rho_f c_f \langle q|grad\ T\rangle = 0 \qquad\qquad 14$$

Where T is the temperature, λ is the hydrodynamic thermal conductivity, $\rho_f c_f$ is the heat capacity of the fluid and q is the Darcy velocity.

3.3.5 Fluid Properties

In this simulation, the temperature dependence of both fluid density and viscosity is critical. The fluid density changes with temperature as:

$$\rho_f(T) = \rho_{ref}(1 - \beta(T - T_{ref})) \hspace{4cm} 15$$

where β is the coefficient of thermal expansion. Similarly, the viscosity of the fluid, $\mu(T)$, has an exponential dependence on temperature:

$$\mu(T) = \mu_0 e^{-\frac{T - T_c}{T_v}} \hspace{4cm} 16$$

These relationships ensure that temperature changes directly affect the fluid's flow behavior through changes in both density and viscosity.

3.4   Case Study

3.4.1 Simulation Setup and Parameters

3.4.1.1 Mesh

The numerical model represents a subsurface system with a depth range of 800 m to 1100 m, where the central part between 900 m and 1000 m was modelled as an aquifer. This aquifer was restricted above and below by aquiclude layers which acted as impermeable confining zones, limiting convective heat transfer to the aquifer. A 50m long heat source was placed at the bottom of the aquifer, at a depth of 1000 m, to simulate thermal energy source to the system, representing a thermal energy storage scenario. The mesh was generated using Gmsh, an open-source mesh generation tool that allowed the creation of structured and unstructured meshes with user-defined resolution(Geuzaine and Remacle, 2009). In this model, a higher resolution was applied around the heat source to accurately capture heat transfer processes and ensure detailed simulation results in areas where more changes are anticipated. The mesh contained separate physical groups defined for each layer (aquiclude and aquifer) and boundary conditions applied to the top, bottom and sides of the model. The mesh was later converted to a VTU format for use in OGS.
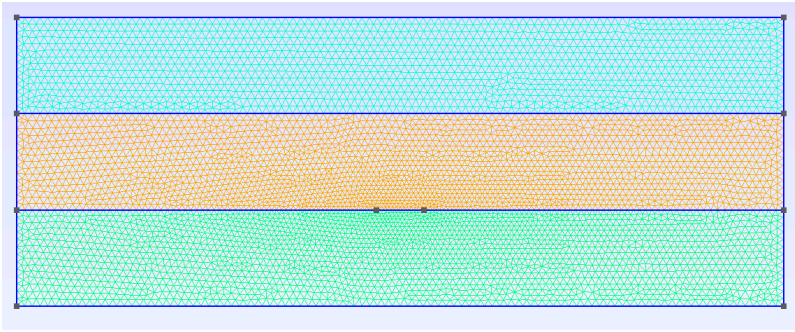
Figure 5 Mesh

3.4.1.2 Boundary and Initial Conditions

The boundary and initial conditions in this OGS model were set up to simulate realistic conditions of the system within an underground aquifer bounded by aquiclude layers. The initial conditions were defined by a temperature gradient reflecting natural geothermal conditions, starting from a surface temperature of 15°C (288.15 K) with a linear increase of 0.03 K/m, resulting in a temperature of 39°C (312.15 K) at a depth of 800 meters. The gradient continued throughout the domain, reaching 48°C (321.15K) at the bottom of the system, simulating geothermal temperature changes with depth. In addition, the initial pressure at the top of the model was set to represent hydrostatic pressure conditions at a depth of 800m.

The boundary conditions were critical in controlling the thermal and flow behavior within the system. At the heat source a Dirichlet boundary condition fixed the temperature at 300°C (573.15 K) to simulate the injection of thermal energy.

For groundwater flow, Neumann boundary conditions were applied along the sides of the aquifer. At the left and right boundaries, these Neumann conditions simulated groundwater flow by prescribing velocities that facilitate lateral movement of water through the aquifer. In the base case the groundwater flow velocity was 3.15 m/year flowing from the left to the right side.

3.4.1.3 Material Properties

To obtain realistic property values for the model, an exploratory literature review was carried out. This review focused on key parameters for claystone and sandstone as well as groundwater flow velocities. The data collected ensured that the model reflects typical geological conditions and provides a solid basis for accurate simulations and sensitivity analysis.

The properties of the sandstone in the base case model were chosen to be temperature dependent to reflect the significant temperature variations within this layer as it serves as the primary

location for the thermal energy storage system. Due to the large temperature differences in the sandstone aquifer, the temperature-dependent behavior of thermal conductivity as well as the specific heat capacity were included to more accurately represent the dynamics of heat transfer. In contrast, the properties of the surrounding aquicludes were kept constant. These claystone layers act primarily as low permeability boundaries, contributing minimally to the overall heat storage and transport, and therefore do not experience significant temperature changes. Therefore, temperature dependence of the properties for the claystone was not considered necessary in the simulation.

In the context of the sandstone aquifer, thermal conductivity values vary significantly depending on the porosity and saturation of the rock. According to experimental data, thermal conductivity values for dry sandstone range from 1.29 to 2.26 W/m-K, while for saturated sandstone they increase to 2.28 to 3.74 W/m-K(Shen *et al.*, 2021).

The study by Emirov et al. (2021) highlights the effect of temperature and pressure on the thermal conductivity of sandstone. As temperature increases, the thermal conductivity decreases, with values dropping from 2.06 W/m-K at 273 K to 1.66 W/m-K at 523 K. This decrease is attributed to the anharmonic scattering of thermal waves (phonons), where higher temperatures increase atomic vibrations, causing more frequent phonon collisions and disrupting heat transfer. This behavior is consistent with materials with crystalline structures, where heat transfer relies on wave-like phonon motion and scattering increases with temperature. Pressure, however, has the opposite effect, increasing thermal conductivity. At high pressures up to 400 MPa, the conductivity rises to 2.95 W/m-K at 273 K. The increase in pressure reduces the interatomic distances, which increases the maximum frequency of atomic vibrations and leads to more efficient heat transfer. In polycrystalline structures such as sandstone, higher pressure also compresses grain boundaries, reducing defects and allowing better phonon propagation through the material, leading to higher thermal conductivity(Emirov *et al.*, 2021).

The study by Jiang et al. (2021) identifies quartz as a key mineral influencing the thermal conductivity of sandstone. The samples with higher quartz content, such as a sample with 50.1% quartz, had the highest thermal conductivity values, reaching 4.15 W/m-K. This is consistent with the thermal properties of quartz, which has a high intrinsic thermal conductivity of 7.8 W/m-K. The presence of quartz in sandstone significantly increases the overall thermal conductivity, as quartz grains act as efficient pathways for heat transfer. The study also shows that as quartz content decreases, thermal conductivity tends to decrease, with other minerals such as clay or calcite, which have lower thermal conductivities, contributing less to heat transfer. The relationship between quartz content and conductivity highlights the significance

of mineral composition in determining the thermal behavior of sedimentary rocks(Jiang *et al.*, 2021).
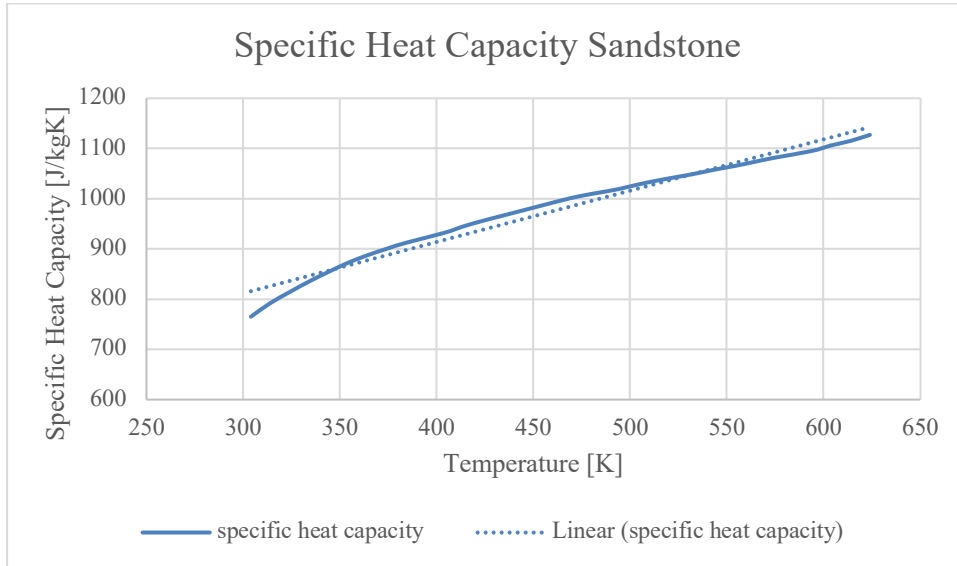
Figure 6 Temperature dependence of Sandstone specific heat capacity and linear trendline

Based on the findings of Emirov et al. (2021), the thermal conductivity of sandstone shows significant variations with both temperature and pressure. While the study provides detailed measurements of thermal conductivity at various pressures ranging from 0.1 MPa to 400 MPa, specific data for 10 MPa pressure were not directly available. To overcome this, interpolated values for the thermal conductivity of dry sandstone at 10 MPa were calculated for temperatures between 273 K and 523 K. A temperature dependent linear function was fitted to these values to capture the temperature dependence in the simulation.
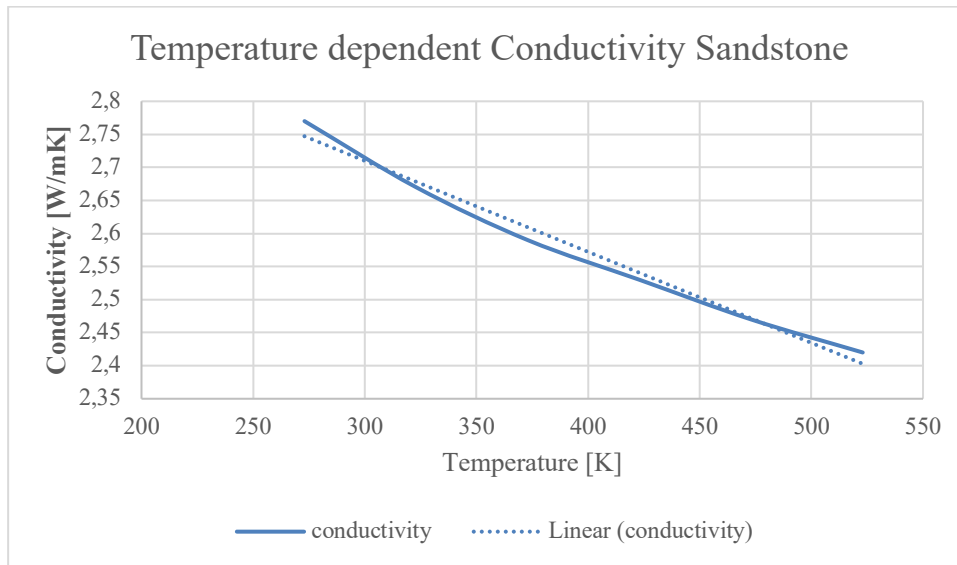
Figure 7 Temperature dependency of Sandstone Conductivity and linear trendline

The specific heat capacities for clay and sandstone used in this sensitivity analysis were taken from Waples and Waples (2004), which provides comprehensive data on the thermal properties of various rock types. According to the reference, the specific heat capacity of clay is 860 J/kg-K and that of sandstone is 775 J/kg-K. Waples and Waples also define specific heat capacity as the amount of energy required to raise the temperature of a unit mass of material by one degree Kelvin, a property that plays a fundamental role in heat transfer processes in porous media. This definition is particularly relevant to thermal energy storage systems, where understanding the heat retention characteristics of aquifer materials is essential for optimizing performance(Waples and Waples, 2004).

In examining the thermal properties of sandstone, the specific heat capacity showed some variation with lithology. Coarse sandstone had specific heat capacities ranging from 816 to 915 J/kg-K, fine sandstone from 787 to 811 J/kg-K and siltstone from 768 to 792 J/kg-K. These variations were mainly influenced by factors such as porosity, mineral composition and density. Higher porosity was associated with a slight increase in specific heat capacity, while density showed a weak negative correlation. Furthermore, the presence of clay minerals and quartz had minimal effect on the specific heat capacity, resulting in relatively stable values across different sandstone types(Xiong *et al.*, 2020).

The specific heat capacity of water was modelled as a temperature dependent property to ensure a more accurate representation of heat transport phenomena. Using CoolProp, a thermophysical property library, the specific heat capacity of water was calculated over a temperature range of 15°C to 300°C (288.15 K to 573.15 K). The resulting data was used to fit a polynomial equation.

This temperature dependence is crucial because the ability of water to store and transfer heat changes with increasing temperature, affecting the efficiency of geothermal systems. The fitted equation was then incorporated into the model to capture the variation in heat capacity with temperature, ensuring that thermal simulations accurately reflect the behavior of water in the subsurface under varying thermal conditions. The same approach was used to obtain temperature dependent conductivity values for water.
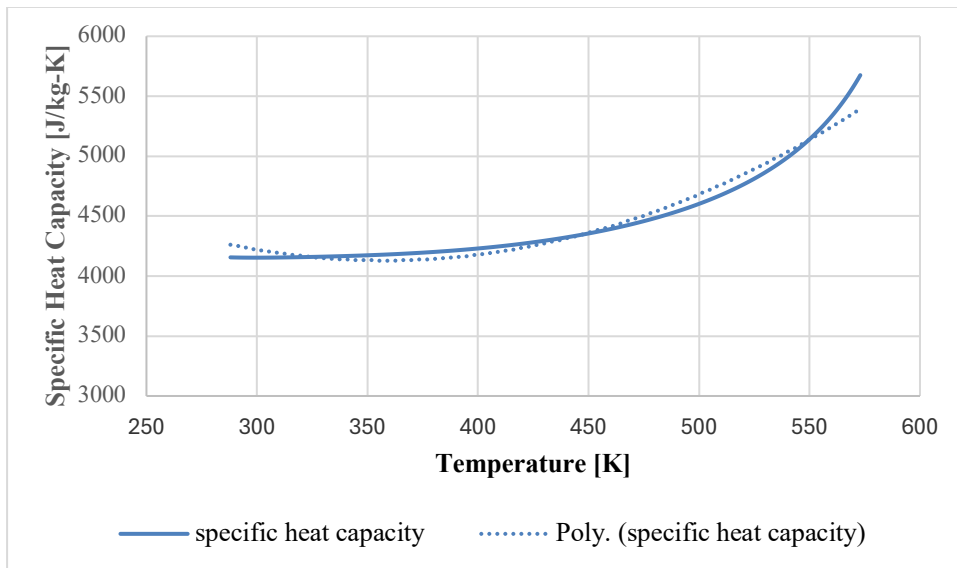
Figure 8 Temperature dependence of Water Specific Heat Capacity and polynomial trendline
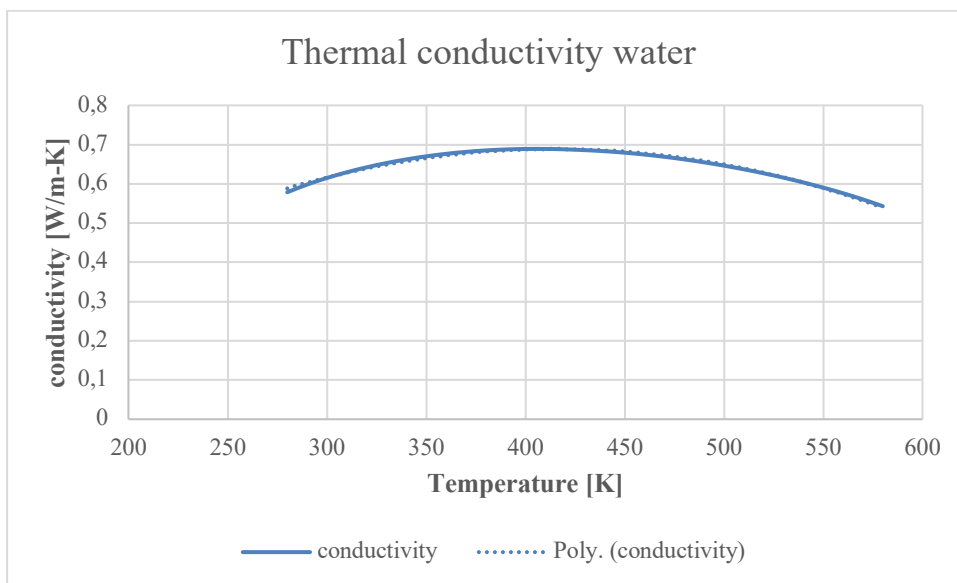
Figure 9 Temperature dependency Thermal Conductivity of Water and polynomial trendline

The thermal conductivity of claystone ranges from 0.66 to 1.23 W/m·K. This variability depends on factors such as mineral composition, porosity, and grain size. Higher clay content generally reduces thermal conductivity due to the fine-grained nature and lower heat transfer efficiency of clay minerals. Conversely, materials with more sand or quartz content tend to have slightly higher conductivity(Midttømme *et al.*, 1998).

The study by Labus and Labus found that the thermal conductivity of claystone varied between 0.80 and 1.25 W/m-K. This variability was related to factors such as mineral composition, particularly the amount of quartz, porosity and the presence of organic matter. Samples with higher quartz content had slightly higher thermal conductivity, while those with more clay or organic material had lower values(Labus and Labus, 2018).

The study of the Mercia Mudstone Group provided comprehensive data on the thermal conductivity of different rock types, including mudstones. The thermal conductivity of mudstones ranges from 1.67 to 2.81 W/m-K, depending on their composition and structural characteristics. The study also notes that silty mudstones generally have slightly lower thermal conductivity values than sandier or quartz-rich mudstones, with silty mudstones ranging from 1.87 to 2.12 W/m-K. The mineralogical composition, particularly the amount of quartz and clay, is important when determining these values. The fine-grained nature of mudstones and the presence of clay minerals reduce their thermal conductivity, as finer particles and clay materials tend to impede heat flow(Parkes *et al.*, 2021).

In OpenGeoSys, thermal porosity mixing was used to automatically calculate the effective thermal conductivity of a porous medium based on the thermal conductivities of its solid and liquid phases together with the porosity. This approach is particularly useful for materials that are completely saturated with water. To model the correct thermal behavior of such materials, the conductivities of both the solid phase and the liquid phase are required. These values are then combined using porosity as a weighting factor to produce a single effective thermal conductivity for the whole medium. This is done using a volumetric mixing rule that averages the conductivities of the phases according to their respective volumes. In OpenGeoSys this is specified using the `EffectiveThermalConductivityPorosityMixing` property, which allows the software to perform the calculation internally once the thermal conductivity of each phase and the porosity have been defined. The volumetric mixing equation is applied as follows:

$$\lambda_{medium} = \lambda_{water} * \phi + \lambda_{clay} * (1 - \phi) \qquad\qquad 17$$

(Naumov *et al.*, 2024)

The permeability and porosity values chosen for the sandstone aquifer in the model were based on experimental data that reflect realistic subsurface conditions. In particular, the study by Li et al. (2023) on the permeability evolution of sandstones provides a comprehensive analysis of how these properties vary under high confining pressures, pore water pressures and elevated temperatures, conditions like those expected in geothermal or energy storage systems. Porosity values in the model range from 9% to 21%, consistent with typical sandstone formations observed in various geological settings. These values represent both denser, more compacted, lower porosity sandstones and more porous, less consolidated sandstones. Such variation allows a realistic representation of the aquifer's storage capacity and fluid flow characteristics. Similarly, the permeability values, ranging from 0.1 mD to 102 mD, 9.869233×10^{-17} to $1.006661766 \times 10^{-13}$ m^2, are informed by the same study. Sandstones with higher porosity tend to have higher permeability, allowing more effective fluid and heat transport, whereas tighter sandstones with lower porosity result in reduced permeability. This range of permeability is critical for simulating groundwater flow and associated thermal convection processes within the aquifer. The study's findings on how permeability decreases with increasing confining pressure are particularly relevant as these conditions are consistent with the depths considered in the model(Li *et al.*, 2023).

The study by Yang and Aplin (2010) provides important insights into the relationship between mudstone porosity and permeability. The permeability of mudstones is highly variable, spanning several orders of magnitude, depending on factors such as clay content and grain size. This variability has important implications for fluid flow and retention in the subsurface. The study finds that mudstone permeabilities range from 2.4×10^{-22} m^2 to 1.7×10^{-16} m^2, while porosities range from 0.04 to 0.78. The authors emphasize that clay content, defined as the fraction of particles less than 2 microns in diameter, plays a critical role in determining both porosity and permeability. At higher clay contents, permeability tends to decrease for the same porosity due to the smaller pore sizes and greater compaction associated with finer grains(Yang and Aplin, 2010).
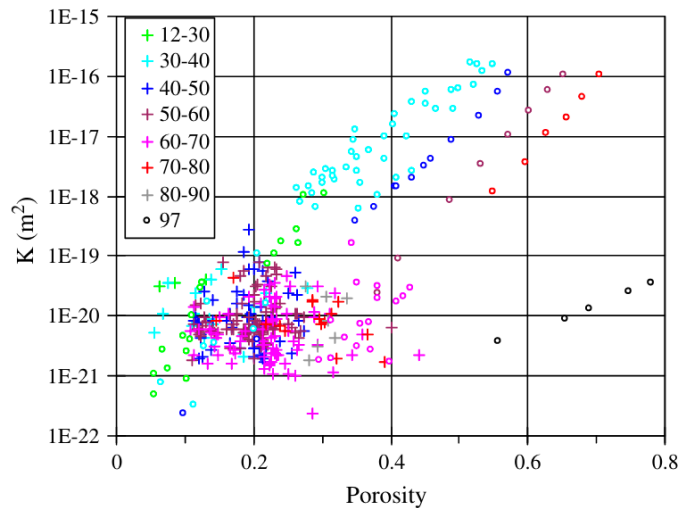
Figure 10 Porosity and Permeability of Mudstone, Clay content in Legend, Circles measured, Crosses modelled (Yang and Aplin, 2010)

Thermal dispersivity is a critical parameter that governs the distribution of heat in an aquifer, combining both conductive and advective processes. In systems such as Aquifer Thermal Energy Storage, heat is transported through both the groundwater and the porous medium. Meaning that the heat transfer mechanism is not solely based on conduction, but is also significantly influenced by dispersion, particularly where groundwater flow is present. Dispersivity is directional, with longitudinal dispersivity - the spreading of heat along the direction of flow - typically greater than transverse dispersivity, which occurs perpendicular to the flow(Vidal *et al.*, 2022). It is generally assumed that the transverse dispersivity is around 10% of the longitudinal dispersivity. Thermal dispersion is a critical factor influencing heat transport within porous media, particularly in the context of aquifers. Thermal dispersion results from the differential advection of heat through the porous media where groundwater flows at different velocities along different pathways. This process enhances heat mixing and affects both the longitudinal and transverse directions of heat transport. The study by Molina et al. (2011) identifies two main scenarios for thermal dispersivity: in homogeneous aquifers, thermal dispersivity depends mainly on the Darcy velocity, resulting in relatively small values. However, in more heterogeneous systems, where dispersion is scale-dependent, longitudinal dispersivity can range from 0.5 m to 2 m and transverse dispersivity from 0.05 m to 0.2 m. The magnitude of thermal dispersion becomes particularly relevant in coarse-grained aquifers, such as those composed of sands and gravels, where higher groundwater flow rates amplify its effects. Neglecting thermal dispersion in such environments can lead to significant underestimation of the spread of temperature plumes, making it an important consideration in aquifer thermal modelling. Thermal dispersion is scale dependent, particularly in relation to the

size of the field scale and the nature of the aquifer. At small scales, such as a few meters, the influence of thermal dispersion may be minimal, particularly in low permeability materials such as fine sand or clay. However, as the field scale increases, the effect of thermal dispersion becomes more pronounced(Molina-Giraldo *et al.*, 2011).

Another study by Engesgaard et al. (1996) focused more on large-scale dispersion in sandy aquifers, investigating longitudinal and transversal dispersivities on a larger scale of up to 1000m. Longitudinal dispersivity values from 1 to 10 m were observed(Engesgaard *et al.*, 1996).

Therefore, an average value of 5 metres was chosen for the base case simulation of the longitudinal dispersivity and, based on the literature, the transverse dispersivity was set at 0.5 metres as it is typically one tenth of the longitudinal value. In order to cover a wide range of thermal dispersivities, the sensitivity analysis investigated both lower values of 1m for the longitudinal dispersivity and 0.1m for the transverse dispersivity, as well as higher values of 10m and 1m respectively. These variations were tested to assess their impact on the behavior of the system, particularly in terms of heat transfer efficiency and distribution within the subsurface. The objective was to understand how different levels of thermal dispersivity affect the distribution of thermal energy within the system, thereby affecting its ability to retain and transfer heat efficiently.

In preparation for the analysis, groundwater flow velocities in aquifers were reviewed to ensure that realistic values were used. Shallow aquifers, such as those in the Upper Rhine Graben, typically have flow velocities of up to 45 mm/year (1.43×10^{-9} m/s). These values reflect natural conditions, which are influenced by regional recharge and geological structures. For simulation, these flow velocities provide a representative basis for evaluating thermal behavior under realistic aquifer flow conditions, ensuring that the analysis is consistent with observed groundwater dynamics(Koltzer *et al.*, 2019).

In the study of groundwater flow variability within a poorly cemented fractured sandstone aquifer, flow velocities were quantified using two primary methods: Active Distributed Temperature Sensing and Passive Flux Meters. The Active Distributed Temperature Sensing method indicated flow velocities ranging from 7 to 60 cm/day, corresponding to approximately 25.55 m/year to 219 m/year (8.10×10^{-7} m/s to 6.94×10^{-6} m/s). The average velocity measured by Active Distributed Temperature Sensing was 23 cm/day, which corresponds to 83.95 m/year (2.66×10^{-6} m/s). The Passive Flux Meters measurements showed lower velocities, ranging from 2 to 11 cm/day, to 7.3 m/year to 40.15 m/year (2.31×10^{-7} m/s to 1.27×10^{-6} m/s). The average velocity recorded by the Passive Flux Meters was 4 cm/day, equivalent to 14.6 m/year

(4.63 x 10^{-7} m/s). These results emphasise the heterogeneity of groundwater flow, with faster flow observed in preferential fracture pathways(Maldaner *et al.*, 2021).

In the East Midlands Triassic Sandstone aquifer, groundwater flow velocities have shown variability over time. Historically, isotopic and geochemical evidence suggests an average velocity of about 0.6 metres per year (1.9 x 10^{-8} m/s) over the last 30,000 years. However, modern flow velocities are lower, averaging 0.2 metres per year (6.3 x 10^{-9} m/s), based on hydraulic gradient and conductivity measurements. The decrease in velocity is attributed to factors such as changes in hydraulic gradients and the degree of confinement within the aquifer, which limit the movement of groundwater downgradient as the flow path deepens and becomes more confined(Edmunds and Smedley, 2000).

Groundwater velocities can vary widely depending on geological conditions and aquifer characteristics. To analyse the effect of velocity on groundwater flow, a higher groundwater velocity was selected for the base case. By selecting a higher velocity, the model emphasises the conductive effects that would be less noticeable at slower flow rates. For the sensitivity analysis, groundwater flow velocities of 0.045 metres per year (1.43 x 10^{-9} m/s) and 7.3 metres per year (2.31 x 10^{-7} m/s) were evaluated. In order to analyze the effects of variations in flow rates on heat propagation. These different flow rates helped to evaluate the response of the system under both slow and moderate groundwater movement conditions, providing a comprehensive understanding of how groundwater velocity affects thermal behaviour in the modelled aquifer.

Chapter 4

Results

4.1   Results and Sensitivity Analysis

The performance of a thermal energy storage system within a geothermal reservoir is highly dependent on several physical parameters, including permeability, porosity, groundwater flow rate, thermal dispersivity, sandstone specific heat capacity and conductivity. These parameters influence the heat transfer mechanisms within the porous medium, affecting both the efficiency of heat storage and the ability to recover stored thermal energy. In such a system, small variations in these parameters can lead to significant differences in the temperature distribution and overall performance of the TES. The sensitivity analysis purpose in this study was to assess how changes in individual variables affect the overall performance and heat distribution in the model. The analysis was carried out using a 'one-at-a-time' approach, where each variable was changed independently while the others are held constant. This allowed the isolated effect analysis of each parameter. Three scenarios were examined: the base case, which represents expected or average conditions; a higher case, where the value of the variable is increased; and a lower case, where the variable is decreased. The range in which each variable changes was chosen based on previous literature review. By comparing these three cases, the effect of varying the parameter were able to be clearly observed, providing an insight into how sensitive the model is to changes in that variable. This method was particularly useful in determining which variables require precise calibration and which have a lesser effect on the model's output.

This sensitivity analysis focused specifically on the rock properties within the aquifer, as this was the primary area where thermal energy storage was concentrated and where heat transfer processes were of most interest. The properties of the surrounding clay layers were assumed to have minimal effect on the heat storage, since they just served as a confining layer in the aquifer and recovery process and therefore their values were held constant throughout the analysis to ensure that only the variations in the aquifer affected the results.

The following table shows the key parameters that were used in the sensitivity analysis of the Thermal Energy Storage system. Each parameter is listed with its corresponding base case value

and the range of variation applied during the analysis. The base case served as a reference point, while the ranges of variation allowed the influence of each parameter on heat distribution, fluid flow and overall system performance to be examined.

Table 1 Input Parameters - Base Case and Sensitivity Analysis

Parameter	Base Case Value	Variation Range	Unit
Permeability k	1×10^{-13}	1×10^{-15} to 1×10^{-12}	m^2
Porosity ϕ	0.1	0.05 to 0.2	-
Groundwater Flow Velocity	1×10^{-7}	1.43×10^{-9} to 2.31×10^{-7}	m/s
Thermal Dispersivity L/T	5/0.5	1/0.1-10/1	m
Sandstone Conductivity	Temperature dependent	2.65 – 4.15	W/m-K
Sandstone Specific Heat Capacity	Temperature dependent	775 - 915	J/kg-K

The energy increase in the aquifer during thermal energy storage operations was evaluated using Equation 18, which calculates the total accumulated thermal energy ΔE within the system. The equation integrates key thermodynamic parameters, such as the density ρ and specific heat capacity c_p of the medium, together with the change in temperature ΔT over the storage volume V, as shown in the following form:

$$\Delta E = \int (\rho c_p \Delta T V)\, d\Omega \qquad\qquad 18$$

In this formulation, V represents the volume of the aquifer, and the integral calculates the amount of thermal energy stored over the entire volume. This is crucial for assessing the efficiency of the system in storing and distributing heat during the operational phase(Chen *et al.*, 2024).

In the case of 2D simulation, this equation was adapted to reflect the two-dimensional nature of the model. Instead of integrating over the volume, the equation was adapted to integrate over the area A of the aquifer. The modified equation in 2D form becomes:

$$\Delta E = \int (\rho c_p \Delta T A)\, d\Omega \qquad\qquad 19$$

This adjustment reflects the simplification required for 2D simulations where heat storage is evaluated over the surface rather than a three-dimensional volume. Despite this simplification, the core principle of evaluating the energy change remains consistent, allowing an accurate estimation of the energy accumulation in the system.

4.1.1 Base Case

The base case aimed to illustrate the heat transport from a 300°C (573.15 K) source within a sandstone aquifer over a 5-year period. Given the significant temperature gradient, this model incorporated temperature dependent properties for both the sandstone and the water. The thermal conductivity and specific heat capacity of the sandstone vary with temperature, reflecting the non-linear behavior of heat transfer at high temperature differentials. Similarly, the properties of water, including viscosity, density and specific heat, varied with temperature to more accurately simulate its response under geothermal conditions.

Moderate values were used for the baseline scenario, representing typical sandstone conditions, and this case serves as a starting point. The subsequent sensitivity analysis explored the influence of variations in these parameters for lower and higher values.

The base case simulation included groundwater flow within the aquifer, which moved horizontally from left to right at a rate of 3.15 meters per year.

Figure 11 depicts the base case across the entire domain following a five-year simulation period. Figure 12 presents a magnified view of the region surrounding the heating rod, aimed at capturing the heated plume in greater detail. The detailed, magnified image was employed throughout the sensitivity analysis to illustrate the propagation of temperature and the heat distribution in the area of the heating rod.
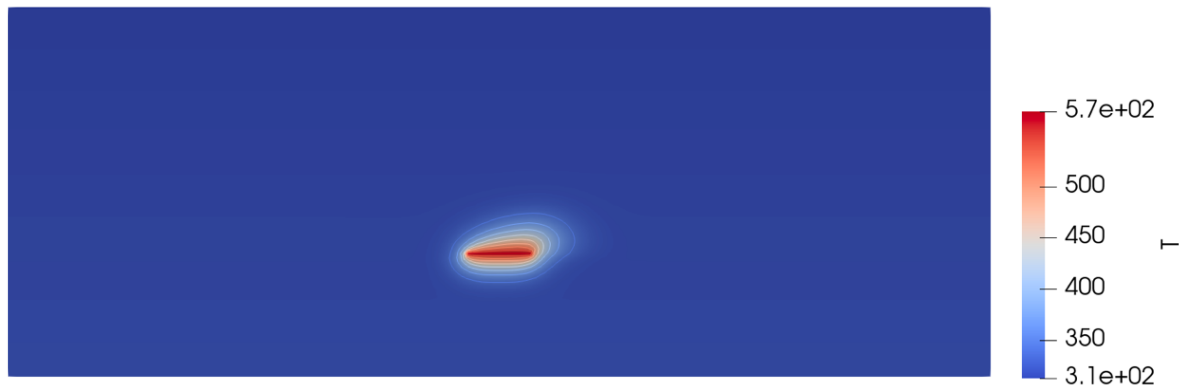
Figure 11 Base Case after 5 years
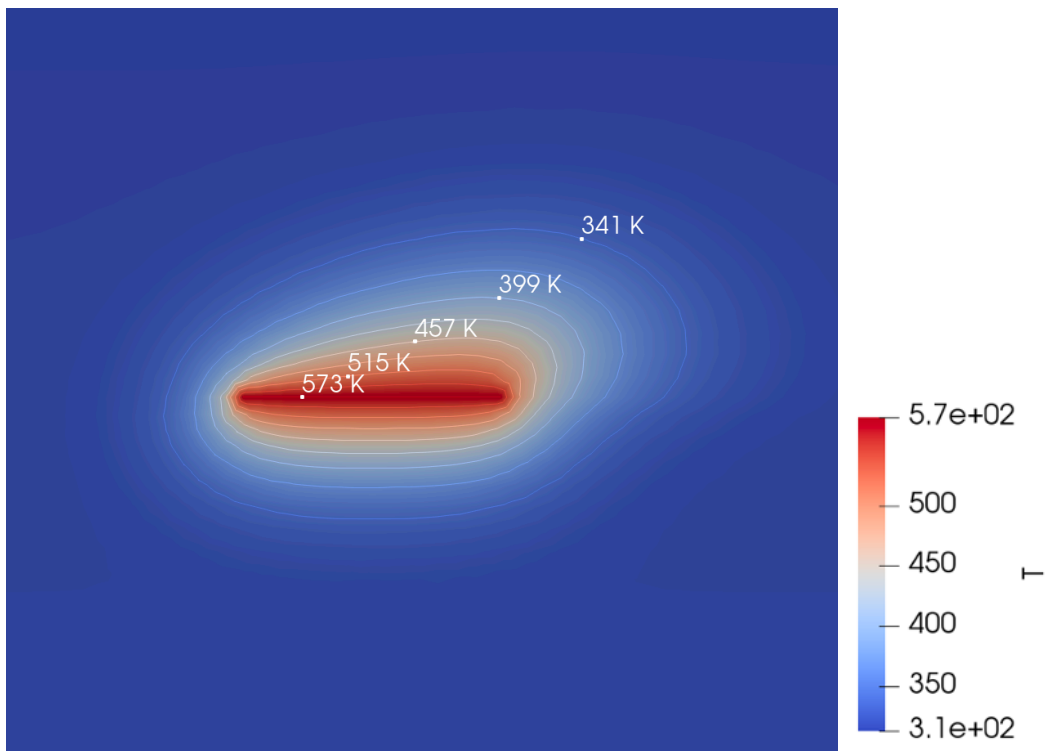
Figure 12 Base case - Temperature distribution around the heat source
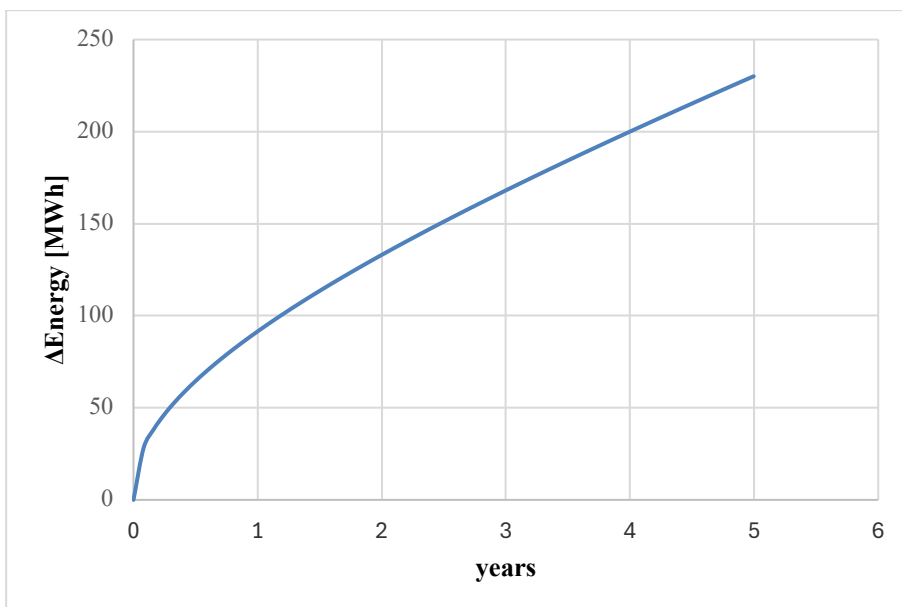
Figure 13 Energy increase over 5 years

Natural convection was expected due to changes in the density of the water as it heats up. Natural convection occurs when the density and viscosity of the heated fluid change, causing buoyancy-driven movement within the system. As the fluid, such as the water in the geothermal

system, is heated, its density decreases, causing the warmer, lighter fluid to rise while the cooler, denser fluid sinks. This creates convective currents that enhance heat transfer. The strength and pattern of this convection are strongly influenced by two dimensionless numbers: the Rayleigh number (Ra) and the Prandtl number (Pr). The Rayleigh number is a significant parameter that describes the ratio of buoyancy forces to the combined effects of thermal diffusion and viscous forces. Higher Rayleigh numbers indicate that buoyancy forces dominate over viscous forces, resulting in stronger convective currents. In the geothermal system, the Rayleigh number increases as the temperature of the water rises, intensifying the convection process and promoting more efficient heat transfer throughout the reservoir. The Prandtl number relates the viscous diffusion of the fluid to its thermal diffusion. A higher Prandtl number indicates that thermal diffusion, or the rate at which heat spreads through the fluid, is slower relative to momentum diffusion. For fluids such as water, which generally have higher Prandtl numbers, this means that while fluid motion can be fast, heat diffusion through the fluid is relatively slow. As a result, convection dominates the heat transfer mechanism in the system, with convective currents playing a greater role in heat distribution than pure conduction. The interaction between these two numbers determines the onset and intensity of natural convection. The higher Rayleigh number due to large temperature gradients will enhance buoyancy-driven flow, while the Prandtl number helps determine how efficiently the heated water transfers energy as it rises and circulates. As both numbers increase with greater temperature gradients, convective heat transfer will intensify, promoting more effective thermal energy storage within the aquifer(Begum *et al.*, 2023).

The base case illustrated a functioning heating system, with the rod reaching its target temperature of 300°C and providing consistent heat to the surrounding environment over a period of 5 years. In the temperature distribution plot, the rod successfully heated the surrounding medium, with the highest temperature concentrated near the heating element, reaching 573.15K (300°C). The temperature decreased radially outwards from the rod, showing heat dissipation by conduction and convection into the surrounding porous medium. The contours of the temperature field show how the heat spreads over time, with a distinct temperature gradient indicating that the heat transfer is governed by the thermal properties of the porous material. The energy accumulation curve shows the total energy absorbed by the system over a 5-year period. At the end of the 5-year period, the total energy accumulated was 230.07 MWh.

4.1.2 Permeability
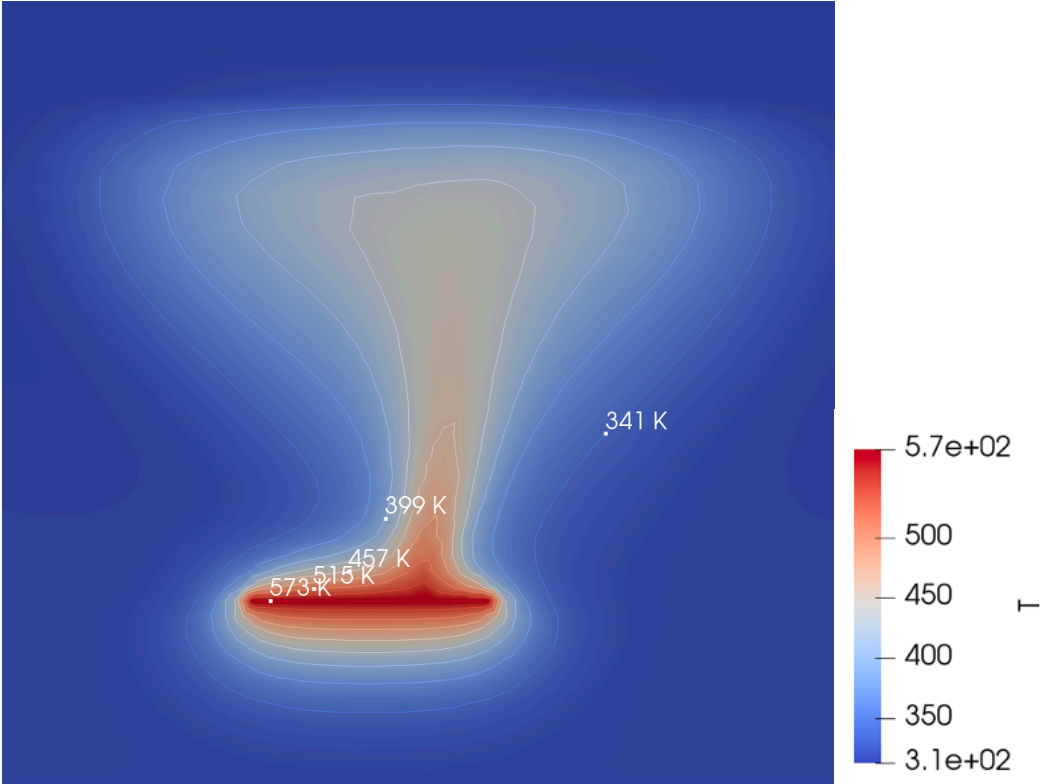
Figure 14 Permeability 10^{-12} m²
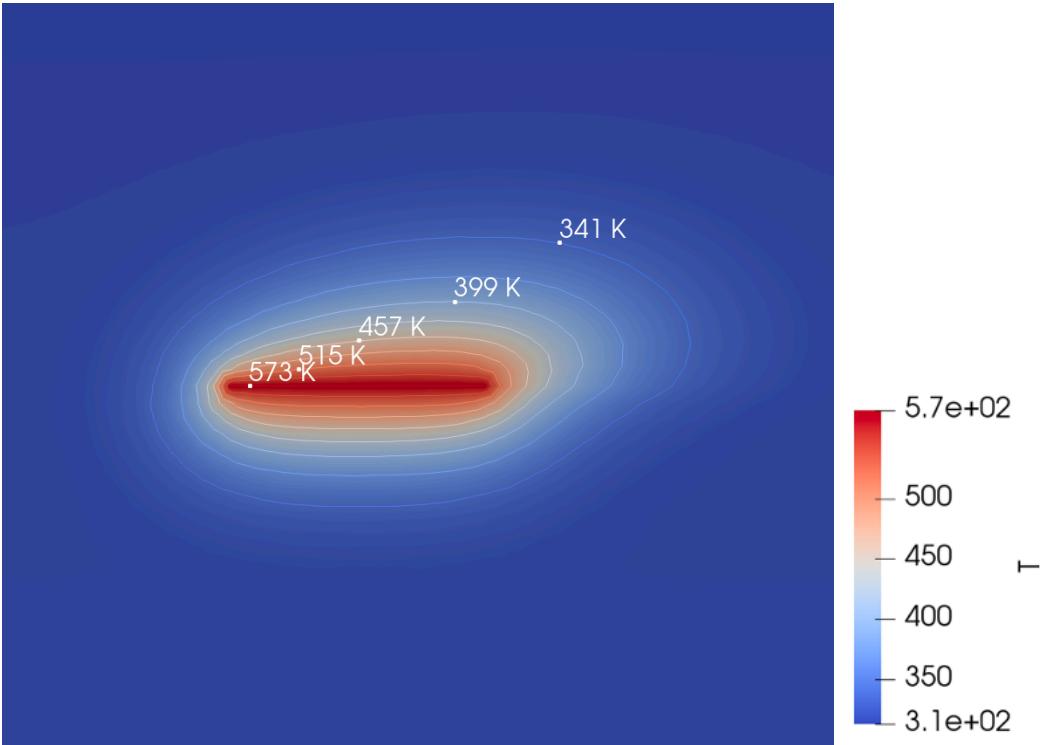
Figure 15 Permeability 10^{-15} m²
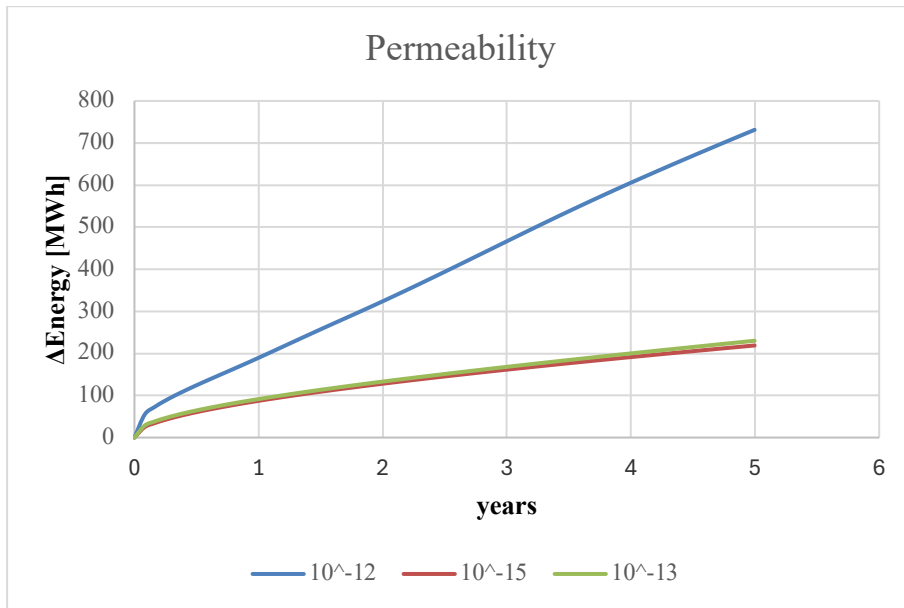
Figure 16 Influence of permeability on energy increase

Table 2 Sensitivity Analysis - Permeability

Permeability [m^2]	ΔEnergy [MWh]
10^{-12}	731.38
10^{-13}	230.07
10^{-15}	218.86

Figure 14 and Figure 15 show an enlarged section of the simulation domain, focusing on the region around the 50m long heat source and extending upwards to the top of the 100m thick aquifer. The area shown highlights the localized thermal effects of the heat source within the aquifer. The pronounced upward movement of heat, represented by the contour lines, illustrates the buoyancy-driven heat plume rising towards the upper boundary of the aquifer due to the lower density of the heated water.

Figure 16 shows the sensitivity of the energy difference over time for three permeability values: 10^{-12} m^2, 10^{-13} m^2 and 10^{-15} m^2. As expected, permeability had a significant effect on the heat transfer through the system, with higher permeability allowing more rapid energy increases.

In the highest permeability case (10^{-12}m^2, blue curve), energy transfer occurred at a much faster rate. This was because high permeability allows for higher fluid flow velocities, which

enhanced convective heat transfer. The rapid transport of heat through the porous medium caused the energy difference to rise steeply with time. In this scenario, convection was the dominant mechanism of heat mechanism, making the system highly sensitive to changes in permeability. In this scenario, the heat plume reached the top of the aquifer, which has a thickness of 100 meters.

For the medium permeability case (10^{-13} m^2, green curve), the system still relied heavily on convection, but the flow velocity was lower due to the reduced permeability. Therefore, the energy transfer rate was slower than in the 10^{-12} m^2 case. However, this permeability was still high enough that convective heat transfer remained effective and the difference in energy transfer rate between 10^{-12} m^2 and 10^{-13} m^2 was noticeable. The energy difference curve rises more slowly than in the case of the highest permeability, but still showed a significant increase. The difference between the 10^{-13}m^2 and 10^{-15}m^2 curves was less significant than the gap between 10^{-12}m^2 and 10^{-13}m^2 due to the decreasing influence of convective heat transfer as permeability decreases.

As the permeability drops below 10^{-16} m^2 the fluid flow is severely restricted, and the system can no longer support effective convective heat transfer. (Scott *et al.*, 2015)

The sensitivity analysis reflected this by the sharp reduction in heat transfer efficiency as permeability decreases. The results of the permeability sensitivity analysis were consistent with established findings that increasing permeability improves heat transfer within a porous medium. As permeability increases, fluid movement through the medium became more efficient, resulting in better heat distribution and convective flow.

4.1.3 Porosity
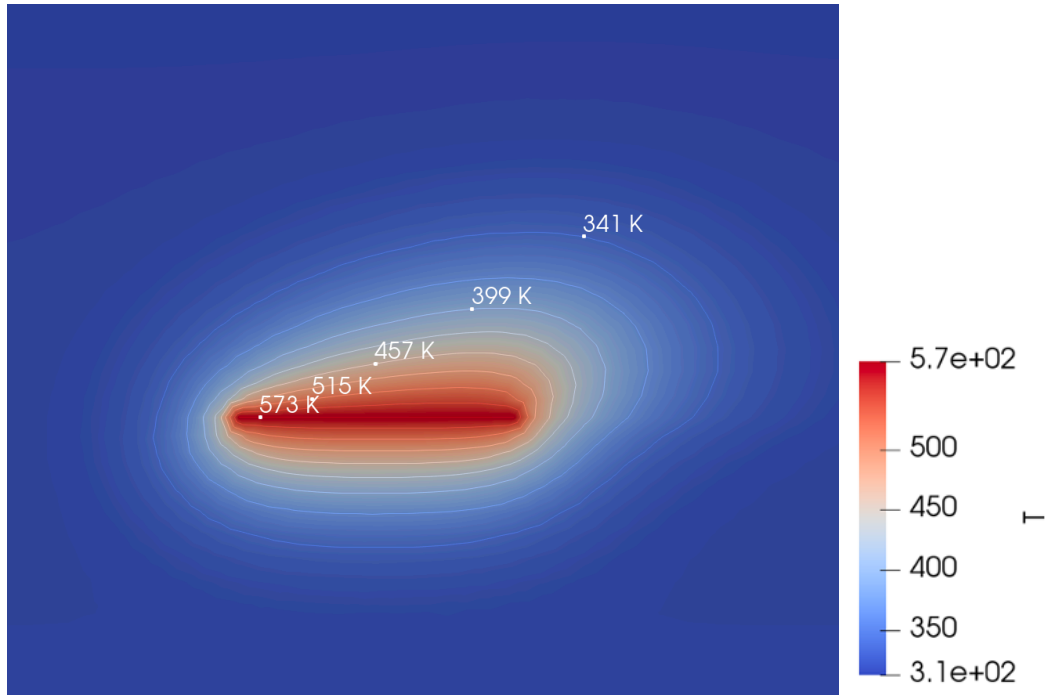
Figure 17 Sandstone Porosity 5%
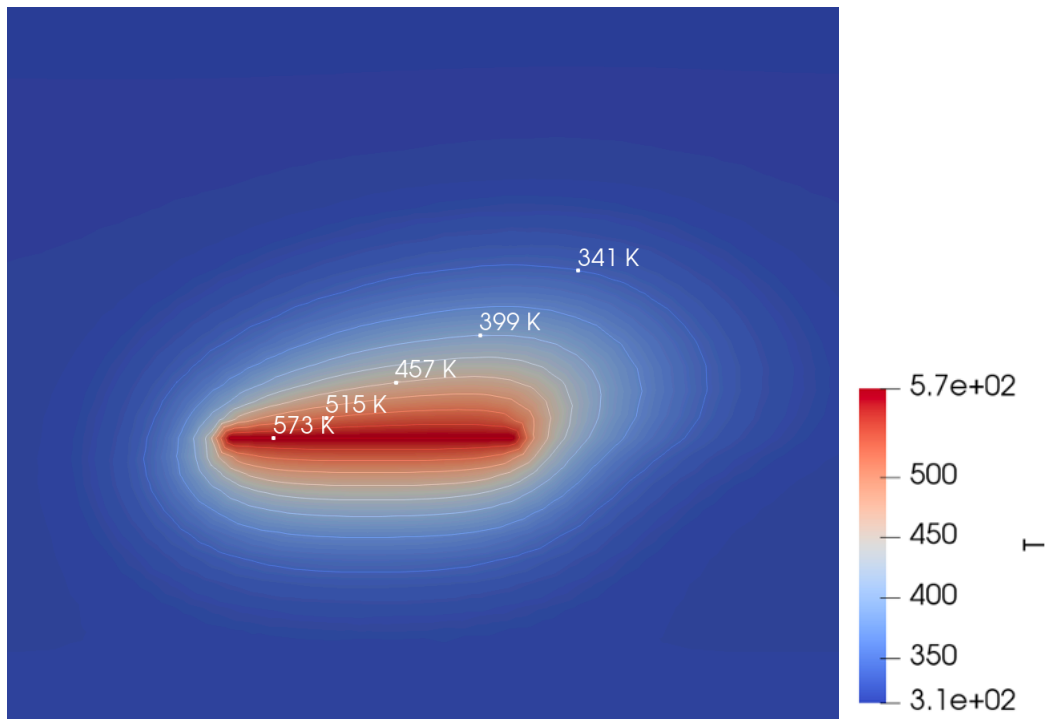
Figure 18 Sandstone Porosity 20%
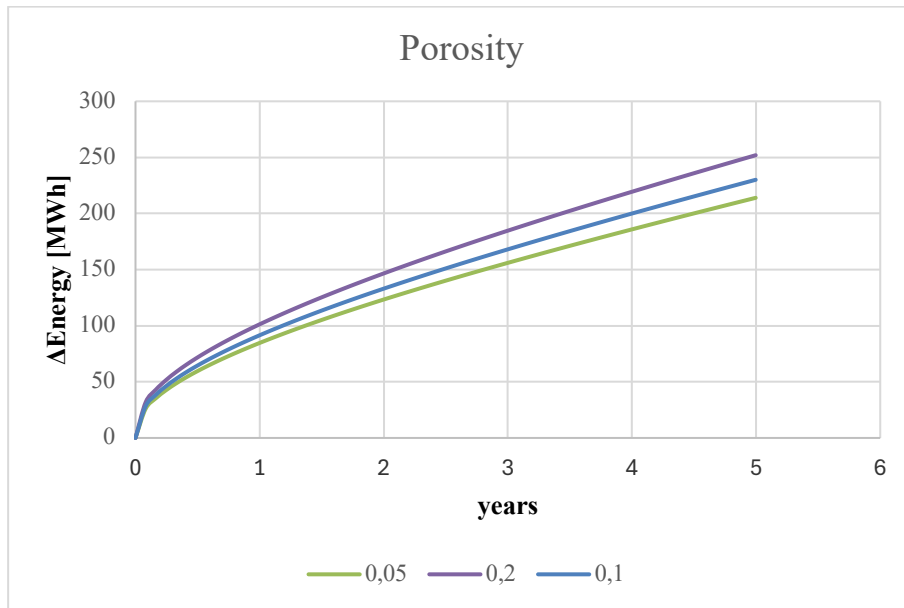
Figure 19 Influence of porosity on energy increase

Table 3 Sensitivity Analysis - Porosity

Porosity [-]	ΔEnergy [MWh]
0.05	213.99
0.1	230.07
0.2	251.97

The porosity sensitivity analysis showed that higher porosity values resulted in greater energy accumulation over time. Though the permeability was constant across the cases, the differences in energy storage can be attributed to the different amounts of water and sandstone present in the porous medium, each with different thermal properties.

The key factors in this result were the thermal conductivity and specific heat capacity of water and sandstone. Water has a much higher specific heat capacity than sandstone which means that it can absorb and store more heat without a significant increase in temperature. In simulations with higher porosity, a larger volume of water was present, allowing more thermal energy to be stored as heat is absorbed by the fluid. This explains why the system with a porosity of 0.2 accumulates the most energy, reaching around 251.97 MWh over 5 years, compared to lower porosities. On the other hand, thermal conductivity played a slightly different role. Sandstone has a higher thermal conductivity than water, which means that heat is conducted

more efficiently through sandstone. At low porosity, the system was dominated by solid phase conduction, which was a less efficient heat transfer mechanism than convection. However, as porosity increased, water occupies a greater proportion of the medium and convective heat transfer within the fluid becomes more prominent. This shift allowed the system to transfer and distribute heat more effectively, despite the lower thermal conductivity of water.

As porosity increased, the role of convection within the fluid becomes critical. Although permeability remained constant in the model, the larger fluid volume at higher porosity allowed more fluid movement, which enhanced convective heat transfer. This convective mechanism is generally more efficient than conduction alone, which explains why energy accumulation improved as porosity increased. The influence of porosity on heat transfer, particularly natural convection, in porous media has been discussed in the literature. As the porosity increases, the flow intensity within the medium also increases due to the buoyancy forces which are acting on the fluid. This leads to a more effective convective heat transfer process as the fluid can move more freely within the porous structure. Specifically, the Alturaihi et al.(2020) study found that higher porosity increases the Nusselt number, a dimensionless measure of heat transfer efficiency, which indicates improved thermal convection around heated surfaces(Alturaihi *et al.*, 2020).

4.1.4 Groundwater Flow Velocity
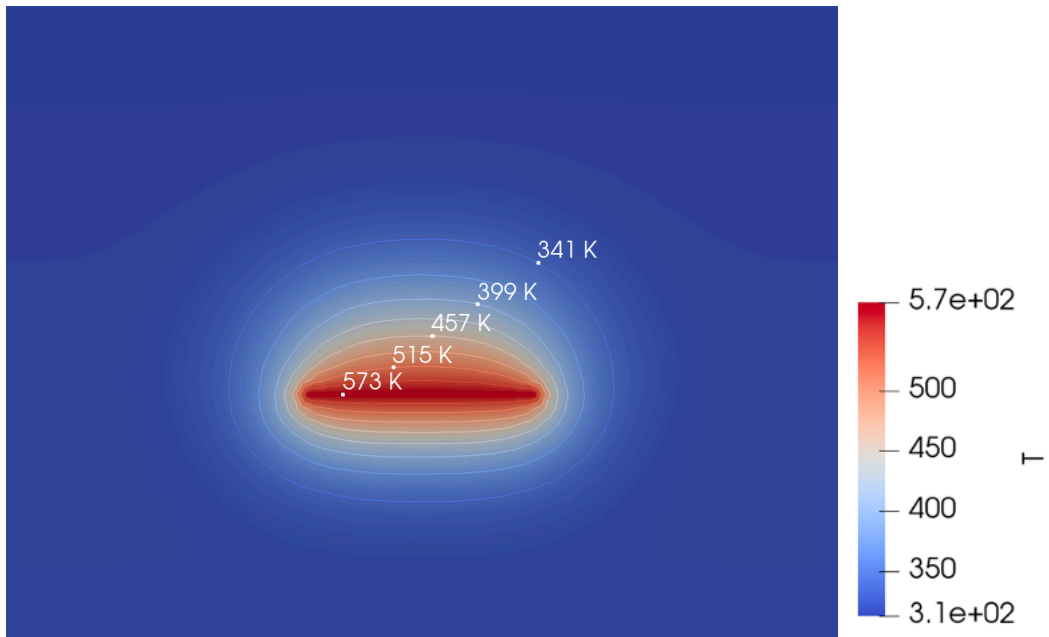
Figure 20 0.045 m/year
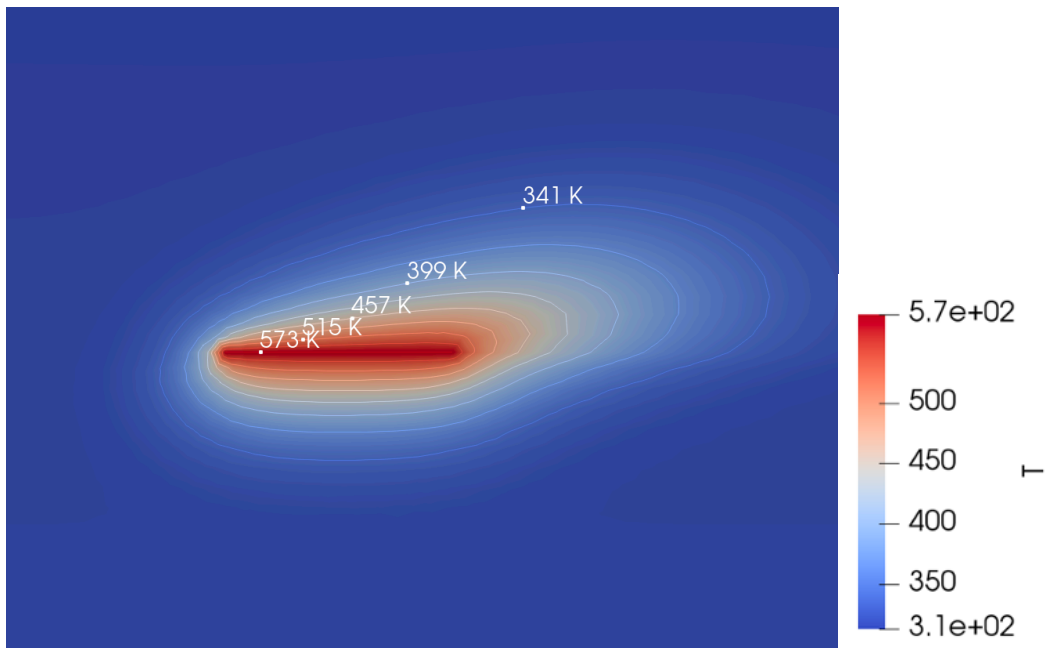
Figure 21 Flow velocity 7.29 m/year
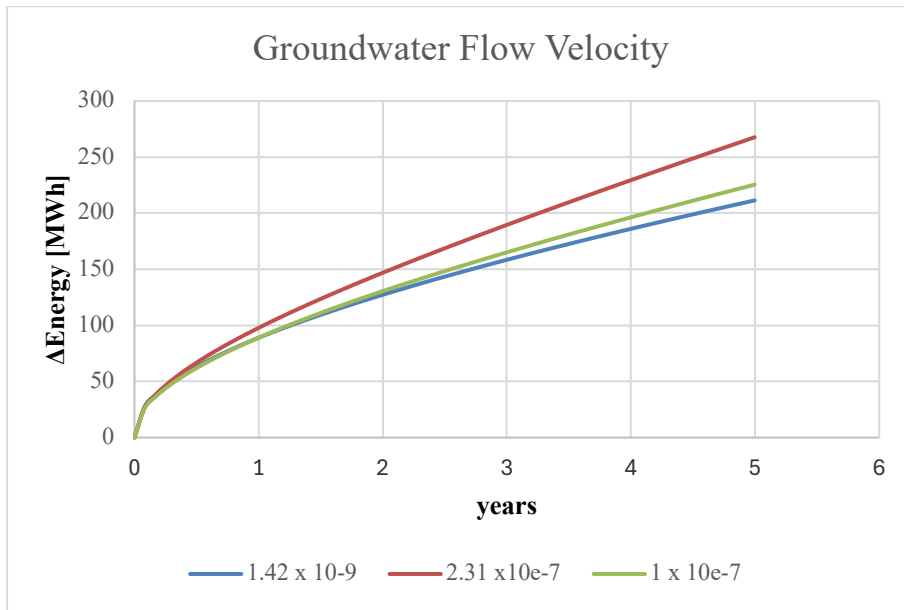
Figure 22 Influence of groundwater flow velocity on energy increase

Table 4 Sensitivity Analysis - Groundwater Flow Velocity

Groundwater Flow Velocity [m/year]	ΔEnergy [MWh]
0.045	226.60
3.15	230.07
7.29	266.18

The sensitivity analysis of the groundwater flow velocity showed a clear relationship between increased flow rates and increased heat transfer within the system, as shown by the total energy accumulation over 5 years. At the lowest groundwater velocity of 0.045 m/year, the stored energy was 226.60 MWh. This accumulation was due to the limited movement of the groundwater, which means that heat transfer relied heavily on conduction rather than convection. In this case, the low velocity of the fluid limited its ability to redistribute heat effectively, resulting in less energy being stored.

As the groundwater velocity increased to 3.15 m/year, the energy storage increased to 230.07 MWh, reflecting the onset of more efficient convective heat transfer. The moderate flow allowed the groundwater to transport heat away from the heat source, which resulted in an

increase in the energy storage capacity of the system. Here convection began to complement conduction, improving heat dissipation and leading to greater energy absorption.

At the highest flow rate of 7.29 m/year, the system accumulated 266.18 MWh over 5 years. The significant increase in energy storage at this velocity was due to the strong advective heat transport facilitated by the higher groundwater flow. As the groundwater moved faster, it was able to transport heat further away from the heat source more efficiently, reducing thermal resistance and preventing the build-up of excess heat around the heat source. This led to a noteworthy improvement in the system's ability to store energy as convection became the dominant heat transfer mechanism. The accelerated rate of groundwater flow resulted in a more extensive dispersion of the heated plume, exceeding 100 meters in horizontal direction.

In summary, the results of the sensitivity analysis confirmed that groundwater flow velocity plays a key role in enhancing heat transfer by advection. As velocity increases, the ability of the system to transport heat increases significantly, allowing for more efficient energy storage. The results were consistent with the general findings that higher groundwater flow rates improve the overall thermal performance of systems such as ground source heat pumps and geothermal energy storage systems. Taking groundwater flow rates in account can therefore lead to better system efficiency and greater energy storage potential(Jia *et al.*, 2022).

4.1.5 Sandstone Specific Heat Capacity
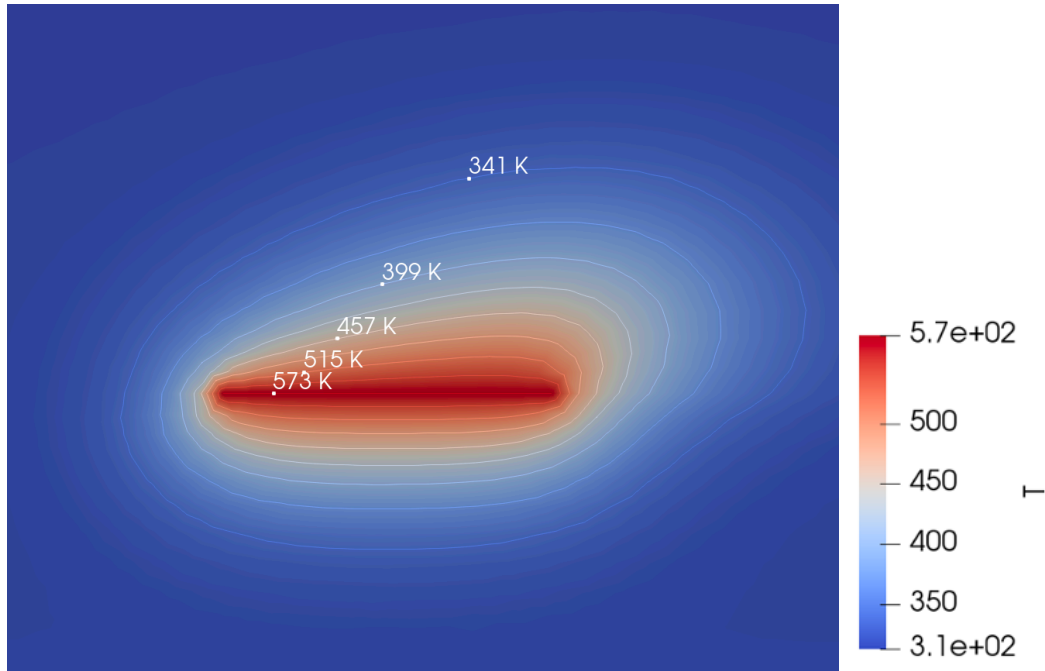
Figure 23 - 775 J/kg K
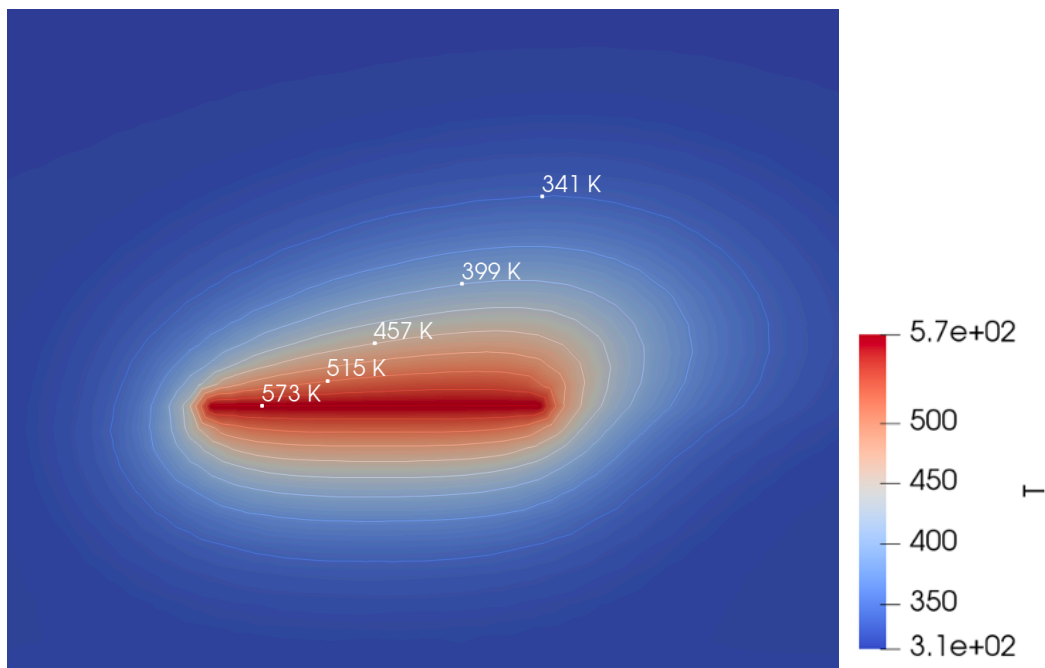
Figure 24 - 915 J/kg K
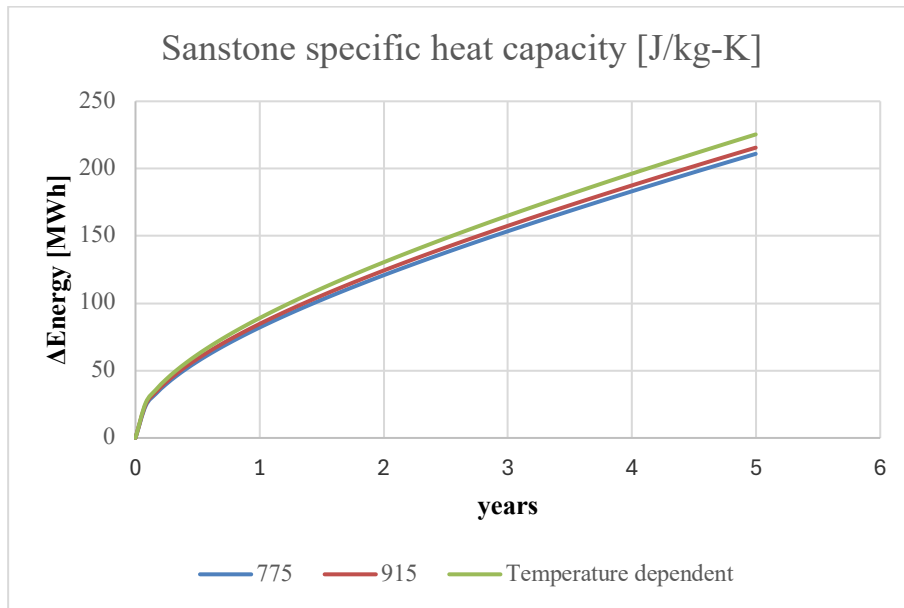
Figure 25 Influence of sandstone specific heat capacity on energy increase

Table 5 - Sensitivity Analysis – specific heat capacity

Sandstone specific heat capacity [J/kg-K]	ΔEnergy [MWh]
775	215.80
Temperature dependent	230.07
915	219.85

The sensitivity analysis of the specific heat capacity of sandstone showed how varying this property affects the system's ability to store energy over time. The analysis compared three cases: a lower specific heat capacity of 775 J/kg-K, a higher value of 915 J/kg-K, and a temperature-dependent specific heat capacity.

For the lower specific heat capacity (775 J/kg-K), the system accumulated 215.80 MWh over the 5-year period. As materials with a lower specific heat require less energy to raise their temperature, the system reached thermal equilibrium faster but stored less total energy. This was expected because sandstone with a lower specific heat cannot absorb as much energy per unit increase in temperature, resulting in less effective long-term energy storage.

With a higher specific heat capacity (915 J/kg-K), the accumulated energy increased to 219.85 MWh. In this case, the sandstone can absorb more heat without a substantial increase in temperature which caused greater energy storage over the same period. This behavior was in line with the basic principles of thermal storage: materials with higher specific heat capacities

take longer amount of time to heat up but retain more energy, making them ideal for applications requiring sustained heat storage.

The most energy, 230.07 MWh, was stored in the system when a temperature dependent specific heat capacity model was used. The temperature dependent curve provided shows that as the temperature increased from 300K to 600K, the specific heat capacity of the sandstone increased from approximately 750 J/kg-K to approximately 1100 J/kg-K. This indicates that as the system operates at higher temperatures, the ability of the sandstone to store energy improves significantly. This behavior was consistent with geological processes where the thermal properties of rocks, including sandstone, can change with temperature, improving heat storage as temperature increases.

This sensitivity analysis highlighted the role of specific heat capacity in determining the energy storage potential of a system. The temperature-dependent specific heat model was found to be the most realistic as it captures the natural variation in the thermal behavior of the sandstone at different temperatures, resulting in more efficient energy storage over time. This was consistent with findings in the literature supporting the use of temperature-dependent thermal properties in models for long-term thermal energy storage in geological formations.

4.1.6 Sandstone Thermal Conductivity
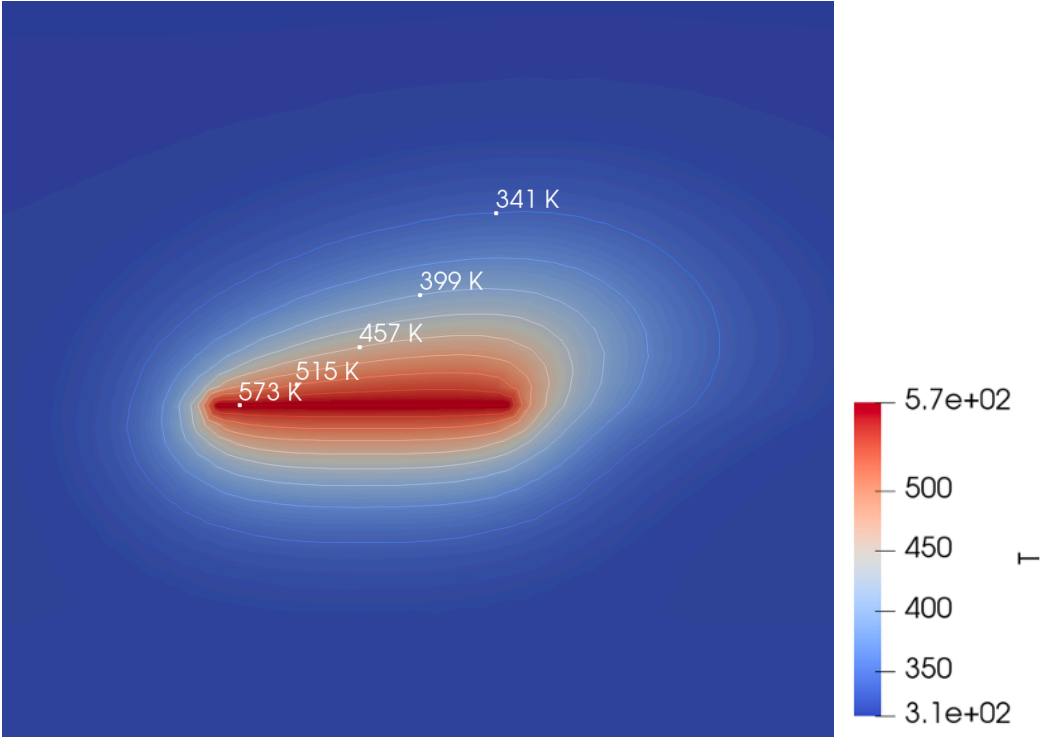
Figure 26 2.65 W/m-K
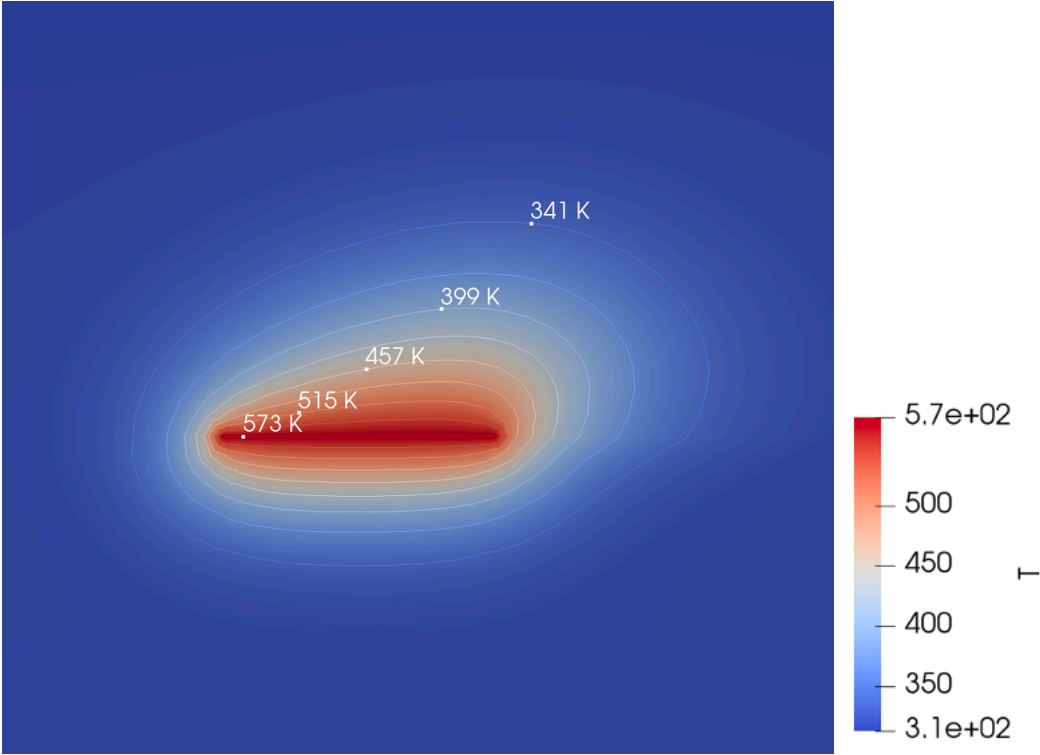
Figure 27 4.15 W/m-K
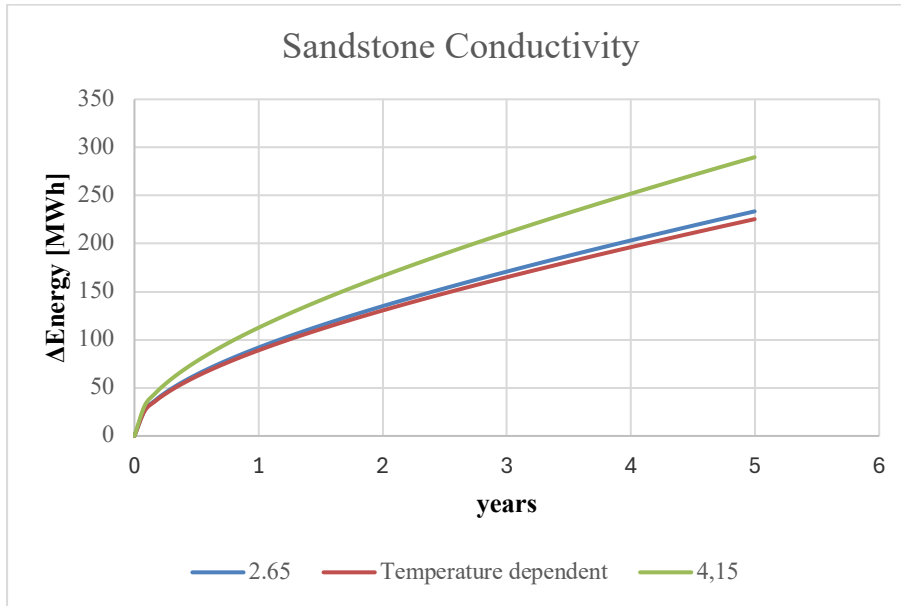
Figure 28 Influence of sandstone conductivity on energy increase

Table 6 - Sensitivity Analysis - Conductivity

Sandstone Conductivity [W/m-K]	ΔEnergy [MWh]
2.65	238.24
Temperature dependent	230.07
4.15	294.47

The thermal conductivity of the sandstones sensitivity analysis showed how different conductivity values affect the energy accumulation of the system over a 5-year period. Three scenarios were compared: a constant conductivity of 2.65 W/m-K, a temperature-dependent conductivity and a higher conductivity of 4.15 W/m-K.

In the first case, with a conductivity of 2.65 W/m-K, the system accumulated 238.24 MWh of energy. The lower thermal conductivity means that heat transfer through the sandstone was lower, resulting in slower heat dissipation. As a result, heat tended to remain localized around the heat source, reducing the total energy absorbed by the system over time.

In the temperature-dependent conductivity scenario, where conductivity decreased with increasing temperature, starting at 2.75 W/m-K and falling to around 2.4 W/m-K at higher temperatures, the system accumulated 230.07 MWh. This behavior reflected the natural tendency of many geological materials, including sandstone, to conduct heat less efficiently at

higher temperatures. As the temperature rose, the decreasing conductivity reduced the heat transfer efficiency slightly, resulting in less energy accumulation compared to the constant 2.65 W/m-K case.

The highest conductivity case, at 4.15 W/m-K, resulted in the greatest energy accumulation, reaching 294.47 MWh. In this scenario, the higher thermal conductivity allowed much more efficient heat transfer through the sandstone. This resulted in enhanced heat dissipation and a greater capacity for the system to store energy.

4.1.7 Thermal Dispersivity
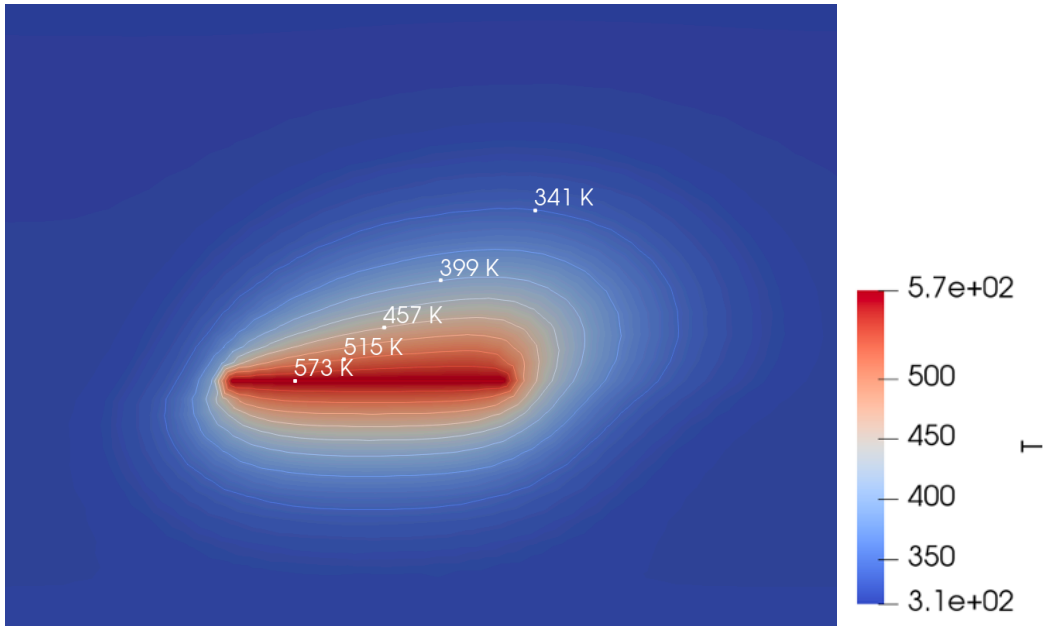
Figure 29 Thermal dispersivity 1/0.1
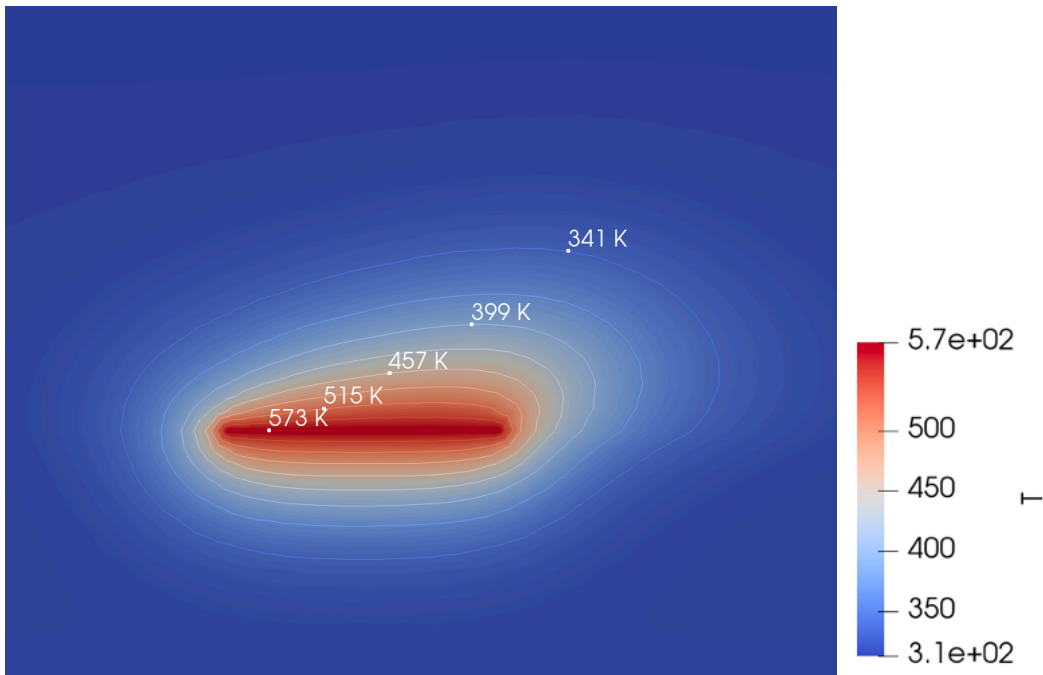
Figure 30 Thermal dispersivity 10/1
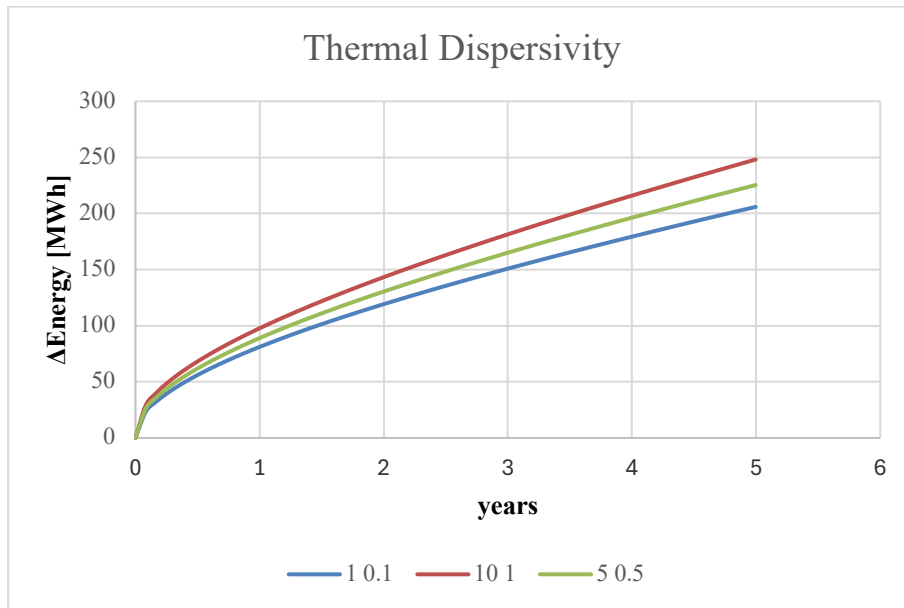
Table 7 Influence of thermal dispersivity on energy increase

Thermal Dispersivity longitudinal/transversal [m]	ΔEnergy [MWh]
1/0.1	207.99
5/0.5	230.07
10/1	254.33

The sensitivity analysis of the thermal dispersivity showed how the longitudinal and transverse dispersivity values affect the systems behavior in terms of temperature and energy increase. Three dispersivity scenarios have been evaluated: 1/0.1 m, 5/0.5 m and 10/1 m, representing the longitudinal and transverse thermal dispersivity, respectively.

In the case of 1/0.1 m dispersivity, the system accumulated 207.99 MWh over the 5 years. This is the scenario with the lowest dispersivity values, both longitudinal and transverse. Lower dispersivity limited the extent to which heat spreads within the medium, resulting in more localized heat retention close to the heat source. The limited spread ensured that more heat remains concentrated, allowing the system to store less energy.

When the longitudinal dispersion was increased to 5 m, the energy storage increases to 230.07 MWh. This increase in longitudinal dispersivity means that heat spreads further in the direction of fluid flow. The faster heat dissipation in the longitudinal direction resulted in higher energy

storage as more heat was propagating away from the heat source and distributed throughout the medium.

In the final case, where both the longitudinal and transverse dispersivity were set to 10 m and 1 m, the system accumulated 254.33 MWh, which is the highest result. In this scenario, although the longitudinal dispersivity allowed the heat to spread far in the direction of flow, the increased transverse dispersivity helped to distribute the heat consistently throughout the medium. The higher transverse dispersivity prevented excessive heat loss in the longitudinal direction by spreading the heat laterally as well, allowing the system to store a higher amount of energy.

It can be said that lower dispersivity values resulted in more localized heat retention and lower energy storage, while increasing longitudinal dispersivity resulted in faster heat dissipation and higher energy storage.

4.1.7.1 Sensitivity Analysis Results - Overview

Table 8 - Overview of sensitivity analysis results

	ΔEnergy [MWh]
Permeability [m^2]	
10^{-12}	731.38
10^{-13}	230.07
10^{-15}	218,86
Porosity [-]	
0.05	213.99
0.1	230.07
0.2	251.97
Groundwater Flow Velocity [m/year]	
0.045	226.60
3.15	230.07
7.29	266.18
Sandstone specific heat capacity [J/kg-K]	
775	215.80
Temperature dependent	230.07
915	219.85
Sandstone Conductivity [W/m-K]	
2.65	238.24
Temperature dependent	230.07
4.15	294.47
Thermal Dispersivity longitudinal/transversal [m]	
1/0.1	207.99
5/0.5	230.07
10/1	254.33

Chapter 5

Discussion

5.1   Discussion

The sensitivity analysis performed on key parameters such as permeability, porosity, groundwater flow velocity, thermal dispersivity, specific heat capacity and thermal conductivity has provided critical insight into the performance of the geothermal system. Each of these parameters affects how heat is transferred and stored in the system.

Permeability was found to be one of the most influential factors in determining heat transfer efficiency. The results indicated that higher permeability significantly increases energy accumulation, up to 731.38 MWh over five years. This result was consistent with previous studies which emphasize that increased permeability enhances convective heat transfer by allowing heat to move more freely through the porous medium. However, as permeability decreases, the system became dominated by conductive heat transfer, resulting in lower energy storage. These results confirmed the critical role of permeability in facilitating effective fluid flow and heat transport in geothermal systems.

Porosity had a similar effect on energy accumulation, with higher porosity values allowing greater heat storage by allowing more water and therefore more convective heat transfer to pass through the system. The results of the porosity sensitivity analysis showed an increase in energy accumulation from 213.99 MWh at a porosity of 0.05 to 251.97 MWh at a porosity of 0.2. These results were consistent with the established understanding that higher fluid content within porous media results in improved heat transfer efficiency by convection.

Groundwater flow velocity also had a significant impact on heat transfer. Higher velocities promoted advective heat transfer, effectively moving heat away from the source. As the groundwater flow velocity increased from 0.045 m/year to 7.29 m/year, the energy

accumulation increased from 226.85 MWh to 266.18 MWh. This is consistent with previous results showing the positive effect of advection on heat dissipation and system performance.

Analysis of the thermal dispersivity showed that lower dispersivity values (1/0.1 m) resulted in more localized heat retention and therefore lower energy storage. However, as the longitudinal dispersivity increased to 5 m, the system experienced a slight increase in energy storage (230.07 MWh) as the heat spreads more rapidly away from the source. When both longitudinal and transverse dispersivity were increased to 10m/1m, the system returned to higher energy storage levels suggesting that balanced heat distribution along both axes is critical.

The specific heat capacity and thermal conductivity of the sandstone were evaluated as temperature dependent parameters, reflecting real geological conditions where these properties vary with temperature. The highest energy storage was observed with a consistently higher thermal conductivity (4.15 W/m-K), which allowed more efficient heat transfer governed by conduction. The system stored 294.47 MWh compared to 230.07 MWh in the temperature-dependent case.

A limitation of this study was the use of two-dimensional simulations to assess energy accumulation. While three-dimensional models would have provided a more comprehensive understanding of heat flow, the primary objective of this study was to assess whether density changes - caused by heating the water - would lead to upward fluid movement and prove the concept of the aquifer heat storage without fluid injection. Given this focus, the use of a 2D model was sufficient to capture the essential dynamics of buoyancy-driven flow and heat transfer, as vertical movement in the system was the critical factor under investigation. Despite this limitation, the 2D model provided a useful initial investigation of heat plume propagation and demonstrated the essential vertical fluid motion driven by buoyancy effects.

5.1.1 Model Performance

The numerical model, built using the OpenGeoSys framework, performed reliably in simulating the key thermal processes within the geothermal aquifer, including both conduction and convection mechanisms. The validation of the model was supported by its foundation on the OpenGeoSys HT benchmark, which ensured that the simulation accurately reflected established heat transfer behavior. Although no direct comparison with field data was available, the model's ability to capture heat conduction through the rock matrix and advective heat transport driven by density changes suggests robust performance. In addition, the inclusion of temperature-dependent material properties, such as thermal conductivity and specific heat capacity, enhanced the realism of the model by reflecting geological responses to temperature changes.

The model was particularly effective in simulating vertical heat transfer driven by density changes in the heated water, resulting in buoyancy-driven upward movement of the fluid. This behavior was essential for understanding the formation and propagation of thermal plumes in the aquifer. The model also successfully demonstrated the role of groundwater flow and rock thermal properties in influencing heat dissipation, particularly in the context of both the aquifer and its surrounding confining layers.

5.2   Future Work

The results of this study offer a solid foundation for further research on geothermal TES, although certain limitations suggest areas for improvement. A key limitation is the use of 2D simulations which, while effective in capturing vertical heat transfer and buoyancy-driven fluid movement, do not fully account for horizontal heat propagation. As a result, the calculated energy storage appears low because it is based on area rather than volume, effectively providing a cross-sectional slice of the reservoir rather than the full volume. Expanding the simulation to 3D would allow a volumetric calculation of stored energy, which would likely result in a significant increase in storage capacity. This move to 3D modelling would allow a more accurate representation of both horizontal and vertical heat flows, providing a comprehensive view of the energy storage potential of the system.

The temperature profile results from this thesis will be used to inform the design and implementation of a system that combines geothermal energy recovery with seasonal thermal storage. These profiles provide critical insights into how heat propagates and is retained in the subsurface, which will guide the optimization of both the storage and recovery phases of the system. By understanding the thermal dynamics through these results, future work can focus on developing a geothermal doublet system that efficiently utilizes the stored heat during the winter months, ensuring effective and sustainable energy recovery.

This temperature profile provides a critical foundation for the next phase of system development, which involves the installation of a geothermal doublet.

When the doublet system is implemented, it is expected that forced convection will significantly improve heat transfer efficiency. The introduction of active fluid flow between the injection and withdrawal wells will amplify the convective forces, allowing faster and more effective distribution of heat throughout the aquifer. As a result, the overall efficiency of the system is expected to improve, with increased fluid flow aiding the recovery of stored thermal energy. Thus, while the current model provides insight into the temperature behavior, the installation of a doublet will transform the system into one where advection-driven convection becomes

the dominant mechanism, allowing for greater heat recovery potential and making the system more comparable to classical ATES systems in terms of performance.

The current results act as a basis for future research aimed at improving the convection and overall energy recovery potential of the system.

Chapter 6

Conclusion

6.1   Summary

In this study, a numerical model was successfully developed using the OpenGeoSys (OGS) framework to simulate the thermal processes in a geothermal aquifer, focusing on both conduction and convection mechanisms. The model effectively captured key dynamics, including buoyancy-driven upward fluid movement due to density changes in heated water, and demonstrated the role of advective heat transfer in improving system efficiency under varying groundwater flow velocities. By incorporating temperature-dependent material properties and simulating heat plumes, the model provided valuable insights into the energy storage and heat dissipation behavior of the system, providing a reliable basis for further optimization and future 3D modelling efforts.

6.2   Evaluation

The primary objective was to develop a numerical model capable of simulating the main thermal processes in a geothermal aquifer, with particular emphasis on heat transfer mechanisms covering conduction, convection and advective transport driven by groundwater flow and density changes of water. This was achieved using the OpenGeoSys framework and the model was validated against the HT benchmark to ensure accuracy and reliability.

One of the reasons why the calculated stored energy appears low is due to the 2D nature of the model, where energy calculations are based on area rather than volume. Consequently, the reported energy values are representative of a cross-sectional slice rather than the full reservoir volume. If the simulation were extended to a 3D model, this would allow a volumetric calculation of the stored energy, significantly increasing the estimated total energy storage.

A potential advantage of the new TES approach over classical ATES is the reduction of heat losses that occurs during the transport of hot water in ATES systems. In ATES, as hot water is injected and moved through the aquifer, thermal dissipation and mixing with cooler water can result in significant losses. In contrast, the TES approach stores heat in situ, minimizing these

transport losses and providing more efficient localized storage. In addition, with ATES, the rise of warmer fluid due to buoyancy can cause the hot water to migrate to different areas of the aquifer, leading to uncertainties in its location at the time of extraction. In the TES system, however, this natural convection is exactly what is desired and is harnessed in the geothermal doublet system to improve heat recovery and ensure more controlled and predictable heat transfer.

References

Alturaihi, M.H., Jassim, L., ALguboori, A.R., Habeeb, J. and Jalghaf, H.K. (2020), "Porosity Influence on Natural Convection Heat Transfer from a Heated Cylinder in a Square Porous Enclosure".

Begum, Z., Saleem, M., Islam, S.U. and Saha, S.C. (2023), "Numerical Study of Natural Convection Flow in Rectangular Cavity with Viscous Dissipation and Internal Heat Generation for Different Aspect Ratios", *Energies*, Vol. 16 No. 14, p. 5267.

Bell, I.H., Wronski, J., Quoilin, S. and Lemort, V. (2014), "Pure and Pseudo-pure Fluid Thermophysical Property Evaluation and the Open-Source Thermophysical Property Library CoolProp", *Industrial & Engineering Chemistry Research*, Vol. 53 No. 6, pp. 2498–2508.

Chen, C., Binder, M., Oppelt, L., Hu, Y., Engelmann, C., Arab, A., Xu, W., *et al.* (2024), "Modeling of heat and solute transport in a fracture-matrix mine thermal energy storage system and energy storage performance evaluation", *Journal of Hydrology*, Vol. 636, p. 131335.

Csanyi, E. and EEP - Electrical Engineering Portal. (2013), "Resistive heating explained in detail".

Edmunds, W.M. and Smedley, P.L. (2000), "Residence time indicators in groundwater: the East Midlands Triassic sandstone aquifer", *Applied Geochemistry*, Vol. 15 No. 6, pp. 737–752.

EEP-Electrical Engineering Portal and Csanyi, E. (2011), "Resistive heating explained in details", *EEP - Electrical Engineering Portal*, 27 July, available at: https://electrical-engineering-portal.com/resistive-heating-explained-in-details (accessed 28 October 2024).

Emirov, S.N., Aliverdiev, A.A., Zarichnyak, Yu.P. and Emirov, R.M. (2021), "Studies of the Effective Thermal Conductivity of Sandstone Under High Pressure and Temperature", *Rock Mechanics and Rock Engineering*, Vol. 54 No. 6, pp. 3165–3174.

Engesgaard, P., Jensen, K.H., Molson, J., Frind, E.O. and Olsen, H. (1996), "Large-Scale Dispersion in a Sandy Aquifer: Simulation of Subsurface Transport of Environmental Tritium", *Water Resources Research*, Vol. 32 No. 11, pp. 3253–3266.

Fischer, T., Naumov, D., Magri, F., Walther, M., Zheng, T. and Kolditz, O. (2017), "OpenGeoSys 6: Implementation of the HT Process".

Geuzaine, C. and Remacle, J.-F. (2009), "Gmsh: a three-dimensional finite element mesh generator with built-in pre- and post-processing facilities", *International Journal for Numerical Methods in Engineering*.

Green, M.A. (2002), "Photovoltaic principles", *Physica E: Low-Dimensional Systems and Nanostructures*, Vol. 14 No. 1–2, pp. 11–17.

Jia, G.S., Ma, Z.D., Xia, Z.H., Wang, J.W., Zhang, Y.P. and Jin, L.W. (2022), "Influence of groundwater flow on the ground heat exchanger performance and ground temperature distributions: A comprehensive review of analytical, numerical and experimental studies", *Geothermics*, Vol. 100, p. 102342.

Jiang, X., Wu, C., Fang, X. and Liu, N. (2021), "A New Thermal Conductivity Estimation Model for Sandstone and Mudstone Based on Their Mineral Composition", *Pure and Applied Geophysics*, Vol. 178 No. 10, pp. 3971–3986.

Kallesøe, A.J., Vangkilde-Pedersen, T., Nielsen, J.E., Bakema, G., Egermann, P., Hahn, F., Guglielmetti, L., *et al.* (2021), "HEATSTORE – Underground Thermal Energy Storage (UTES) – State of the Art, Example Cases and Lessons Learned".

Kannan, N. and Vakeesan, D. (2016), "Solar energy for future world: - A review", *Renewable and Sustainable Energy Reviews*, Vol. 62, pp. 1092–1105.

Koltzer, N., Scheck-Wenderoth, M., Cacace, M., Frick, M. and Bott, J. (2019), "Regional hydraulic model of the Upper Rhine Graben", *Advances in Geosciences*, Vol. 49, pp. 197–206.

Labus, M. and Labus, K. (2018), "Thermal conductivity and diffusivity of fine-grained sedimentary rocks", *Journal of Thermal Analysis and Calorimetry*, Vol. 132 No. 3, pp. 1669–1676.

Li, Y., Wu, Y., Qiao, W., Zhang, S. and Li, X. (2023), "The Permeability Evolution of Sandstones with Different Pore Structures under High Confining Pressures, High Pore Water Pressures and High Temperatures", *Applied Sciences*, Vol. 13 No. 3, p. 1771.

Maldaner, C.H., Munn, J.D., Green, B.A., Warner, S.L., Chapman, S.W., Ashton, A., Daubert, L., *et al.* (2021), "Quantifying groundwater flow variability in a poorly cemented fractured sandstone aquifer to inform in situ remediation", *Journal of Contaminant Hydrology*, Vol. 241, p. 103838.

Midttømme, K., Roaldset, E. and Aagaard, P. (1998), "Thermal conductivity of selected claystones and mudstones from England", *Clay Minerals*, Vol. 33 No. 1, pp. 131–145.

Molina-Giraldo, N., Bayer, P. and Blum, P. (2011), "Evaluating the influence of thermal dispersion on temperature plumes from geothermal systems using analytical solutions", *International Journal of Thermal Sciences*, Vol. 50 No. 7, pp. 1223–1231.

Naumov, D., Bilke, L., Lehmann, C., Fischer, T., Wang, W., Shao, H., Buchwald, J., *et al.* (2024), "OpenGeoSys", Zenodo, 4 September, available at:https://doi.org/10.5281/ZENODO.13685289.

Parkes, D., Busby, J., Kemp, S.J., Petitclerc, E. and Mounteney, I. (2021), "The thermal properties of the Mercia Mudstone Group", *Quarterly Journal of Engineering Geology and Hydrogeology*, Vol. 54 No. 2, pp. qjegh2020-098.

Sarbu, I. and Sebarchievici, C. (2018), "A Comprehensive Review of Thermal Energy Storage", *Sustainability*, Vol. 10 No. 1, p. 191.

Scott, S., Driesner, T. and Weis, P. (2015), "Geologic controls on supercritical geothermal resources above magmatic intrusions", *Nature Communications*, Vol. 6 No. 1, p. 7837.

Shen, Y., Wang, X., Wang, Y., Zhou, K., Zhang, J., Zhang, H. and Li, J. (2021), "Thermal conductivity models of sandstone: applicability evaluation and a newly proposed model", *Heat and Mass Transfer*, Vol. 57 No. 6, pp. 985–998.

Stoppato, A. and Benato, A. (2017), "The Importance of Energy Storage", *Energy Storage*.

Usman, Z., Tah, J., Abanda, H. and Nche, C. (2020), "A Critical Appraisal of PV-Systems' Performance", *Buildings*, Vol. 10 No. 11, p. 192.

Vidal, R., Olivella, S., Saaltink, M.W. and Diaz-Maurin, F. (2022), "Heat storage efficiency, ground surface uplift and thermo-hydro-mechanical phenomena for high-temperature aquifer thermal energy storage", *Geothermal Energy*, Vol. 10 No. 1, p. 23.

Waples, D.W. and Waples, J.S. (2004), "A Review and Evaluation of Specific Heat Capacities of Rocks, Minerals, and Subsurface Fluids. Part 1: Minerals and Nonporous Rocks", *Natural Resources Research*, Vol. 13 No. 2, pp. 97–122.

Xiong, J., Lin, H., Ding, H., Pei, H., Rong, C. and Liao, W. (2020), "Investigation on thermal property parameters characteristics of rocks and its influence factors", *Natural Gas Industry B*, Vol. 7 No. 3, pp. 298–308.

Yang, Y. and Aplin, A.C. (2010), "A permeability–porosity relationship for mudstones", *Marine and Petroleum Geology*, Vol. 27 No. 8, pp. 1692–1697.

Zhang, Y., Liu, Y., Bian, K., Zhou, G., Wang, X. and Wei, M. (2024), "Development status and prospect of underground thermal energy storage technology".

Zhou, X. (2021), "Large scale underground seasonal thermal energy storage in China", *Journal of Energy Storage*.

List of Figures

List of Tables

Nomenclature

T	Temperature	[K]
K	Thermal Conductivity	[W/m-K]
c	Fluid velocity	[m/s]
c_p	Specific heat capacity	[J/kg-K]
ϕ	Porosity	[-]
κ	permeability	[m^2]
μ	viscosity	[Pas]
p	Pressure	[Pa]
g	Gravitational acceleration	[m/s^2]
ρ	Density	[kg/m³]

Abbreviations

ATES	Aquifer Thermal Energy Storage
BHE	Borehole Heat Exchanger
BTES	Borehole Thermal Energy Storage
CTES	Cavern Thermal Energy Storage
TES	Thermal Energy Storage
UTES	Underground Thermal Energy Storage
PTES	Pit Thermal Energy Storage
MTES	Mine Thermal Energy Storage
OGS	OpenGeoSys
HT	Hydro-Thermal
PV	Photovoltaic